GEOSPHERE

GEOSPHERE; v. 14, no. 3

doi:10.1130/GES01578.1

10 figures; 3 tables

CORRESPONDENCE: pritchard@cornell.edu

CITATION: Pritchard, M.E., de Silva, S.L., Michelfelder, G., Zandt, G., McNutt, S.R., Gottsmann, J., West, M.E., Blundy, J., Christensen, D.H., Finnegan, N.J., Minaya, E., Sparks, R.S.J., Sunagua, M., Unsworth, M.J., Alvizuri, C., Comeau, M.J., del Potro, R., Díaz, D., Diez, M., Farrell, A., Henderson, S.T., Jay, J.A., Lopez, T., Legrand, D., Naranjo, J.A., McFarlin, H., Muir, D., Perkins, J.P., Spica, Z., Wilder, A., and Ward, K.M., 2018, Synthesis: PLUTONS: Investigating the relationship between pluton growth and volcanism in the Central Andes: Geosphere, v. 14, no. 3, p. 954–982, doi:10.1130/GES01578.1.

Science Editor: Raymond M. Russo

Received 16 June 2017
Revision received 30 November 2017
Accepted 21 February 2018
Published online 29 March 2018

Synthesis: PLUTONS: Investigating the relationship between pluton growth and volcanism in the Central Andes

M.E. Pritchard[1,2], S.L. de Silva[3], G. Michelfelder[4], G. Zandt[5], S.R. McNutt[6], J. Gottsmann[2], M.E. West[7], J. Blundy[2], D.H. Christensen[7], N.J. Finnegan[8], E. Minaya[9], R.S.J. Sparks[2], M. Sunagua[10], M.J. Unsworth[11], C. Alvizuri[7], M.J. Comeau[12], R. del Potro[2], D. Díaz[13], M. Diez[2], A. Farrell[6], S.T. Henderson[1,14], J.A. Jay[15], T. Lopez[7], D. Legrand[16], J.A. Naranjo[17], H. McFarlin[6], D. Muir[18], J.P. Perkins[19], Z. Spica[20], A. Wilder[21], and K.M. Ward[22]

[1]Department of Earth and Atmospheric Sciences, Cornell University, Ithaca, New York 14853, USA
[2]School of Earth Sciences, University of Bristol, BS8 1RJ, United Kingdom
[3]College of Earth, Ocean, and Atmospheric Science, Oregon State University, Corvallis, Oregon 97331, USA
[4]Department of Geography, Geology and Planning, Missouri State University, 901 S. National Ave, Springfield, Missouri 65897, USA
[5]Department of Geosciences, The University of Arizona, 1040 E. 4th Street, Tucson, Arizona 85721-0001, USA
[6]School of Geosciences, University of South Florida, 4202 E. Fowler Avenue, Tampa, Florida 33620, USA
[7]Geophysical Institute, University of Alaska, Fairbanks, 903 N. Koyukuk Drive, Fairbanks, Alaska 99709, USA
[8]Department of Earth and Planetary Sciences, University of California, Santa Cruz, 1156 High Street, Santa Cruz, California 95064, USA
[9]Observatorio San Calixto, Calle Indaburo 944, Casilla 12656, La Paz, Bolivia
[10]Empresa Kawsaqi, Correo Central, La Paz, Bolivia
[11]Department of Physics, University of Alberta, Edmonton, Alberta T6E 2E1, Canada
[12]Institut für Geophysik, Universität Münster, Münster, 48149, Germany
[13]Departamento de Geofísica, Universidad de Chile and Centro de Excelencia en Geotermia de Los Andes, Santiago, Chile
[14]Department of Earth and Space Sciences, University of Washington, Seattle, Washington 98195-1310, USA
[15]2920 Amberleigh Way, Fairfax, Virginia 22031, USA
[16]Instituto de Geofísica, Universidad Nacional Autónoma de México, Av. Universidad 3000, Coyoacán, CP 04510, México DF, Mexico
[17]Servicio Nacional de Geología y Minería, Av. Santa María 0104, Santiago, Chile
[18]School of Earth and Ocean Sciences, Cardiff University, CF10 3AT, United Kingdom
[19]United States Geological Survey, 345 Middlefield Road, Menlo Park, California 94025, USA
[20]Department of Geophysics, Stanford University, 397 Panama Mall, Mitchell Bldg., Stanford, California 94305, USA
[21]1220 SW 3rd Avenue, Suite 1010, Portland, Oregon 97220, USA
[22]Department of Geology and Geophysics, The University of Utah, 115 South 1460 East, Salt Lake City, Utah 84112, USA

ABSTRACT

The Central Andes is a key global location to study the enigmatic relation between volcanism and plutonism because it has been the site of large ignimbrite-forming eruptions during the past several million years and currently hosts the world's largest zone of silicic partial melt in the form of the Altiplano-Puna Magma (or Mush) Body (APMB) and the Southern Puna Magma Body (SPMB). In this themed issue, results from the recently completed PLUTONS project are synthesized. This project focused an interdisciplinary study on two regions of large-scale surface uplift that have been found to represent ongoing movement of magmatic fluids in the middle to upper crust. The locations are Uturuncu in Bolivia near the center of the APMB and Lazufre on the Chile-Argentina border, on the edge of the SPMB. These studies use a suite of geological, geochemical, geophysical (seismology, gravity, surface deformation, and electromagnetic methods), petrological, and geomorphological techniques with numerical modeling to infer the subsurface distribution, quantity, and movements of magmatic fluids, as well as the past history of eruptions. Both Uturuncu and Lazufre show separate geophysical anomalies in the upper, middle, and lower crust (e.g., low seismic velocity, low resistivity, etc.) indicating multiple distinct reservoirs of magma and/or hydrothermal fluids with different physical properties. The characteristics of the geophysical anomalies differ somewhat depending on the technique used—reflecting the different sensitivity of each method to subsurface melt (or fluid) of different compositions, connectivity, and volatile content and highlight the need for integrated, multidisciplinary studies. While the PLUTONS project has led to significant progress, many unresolved issues remain and new questions have been raised.

INTRODUCTION

Crustal magmatism plays a fundamental role in the generation of continental crust and the thermal and rheological evolution of mountain belts and plateaus (e.g., Hamilton and Myers, 1967; Fyfe, 1973; Brown, 2001). Magmas resulting from the chemical differentiation of mantle-derived magmas coupled with crustal partial melting are manifest as granite batholiths and large-volume volcanic eruptions (ignimbrites and their associated calderas). While there is compelling evidence that some large silicic ignimbrites are related to pluton-scale granite magmatic systems (e.g., Lipman, 1984; Chappell et al., 1987),

there is controversy over whether the intrusive and extrusive processes occur simultaneously or indeed are related at all (e.g., Bachmann et al., 2007; Miller et al., 2011; Lundstrom and Glazner, 2016). For example, if large ignimbrite eruptions empty their magma chambers, an equivalent intrusion might not be formed (e.g., Glazner et al., 2004). Also, large magma chambers might grow without eruption (e.g., Jellinek and DePaolo, 2003; de Silva and Gregg, 2014; Cao et al., 2016). Intrusions may grow too slowly to form chambers of eruptible magma (Annen, 2009).

There are few examples of both plutonic and volcanic systems of similar age in the same area, although there are some, such as the Southern Rocky Mountain volcanic field (e.g., Lipman and Bachmann, 2015), the Kohistan arc, Pakistan (e.g., Jagoutz and Schmidt, 2012), and the Yerington batholith, Nevada (Dilles and Wright, 1988). Granite plutons are the integrated result of intrusion over hundreds of thousands to millions of years (e.g., Hamilton and Myers, 1967; Glazner et al., 2004; Paterson et al., 2011) and are typically studied as fossil systems exposed by erosion and tectonic exhumation. Volcanic products provide information on a large magma body at a single moment in time but typically have been eroded away when the intrusions are exposed.

The international PLUTONS project investigated the relationship between presumed ongoing intrusion within the middle to upper crust at two little-studied areas in the Central Andes and past, present, and future volcanism through multidisciplinary observations and numerical modeling. The two focus sites (Uturuncu and Lazufre, Fig. 1A) exhibit persistent uplift at a rate of 1–2 cm/yr and are unusual (e.g., compared to the compilation of calderas in Ruch et al., 2008 and 220 globally deforming volcanoes by Biggs and Pritchard, 2017) in that they are >40 km in diameter, and deformation has persisted for ten or more years. Enigmatically, the uplift centers are not directly below volcanoes with Holocene eruptions. Yet, they are near geophysically imaged zones of partial melt (Fig. 1B; Delph et al., 2017; Ward et al., 2017) and regions of Pleistocene volcanism.

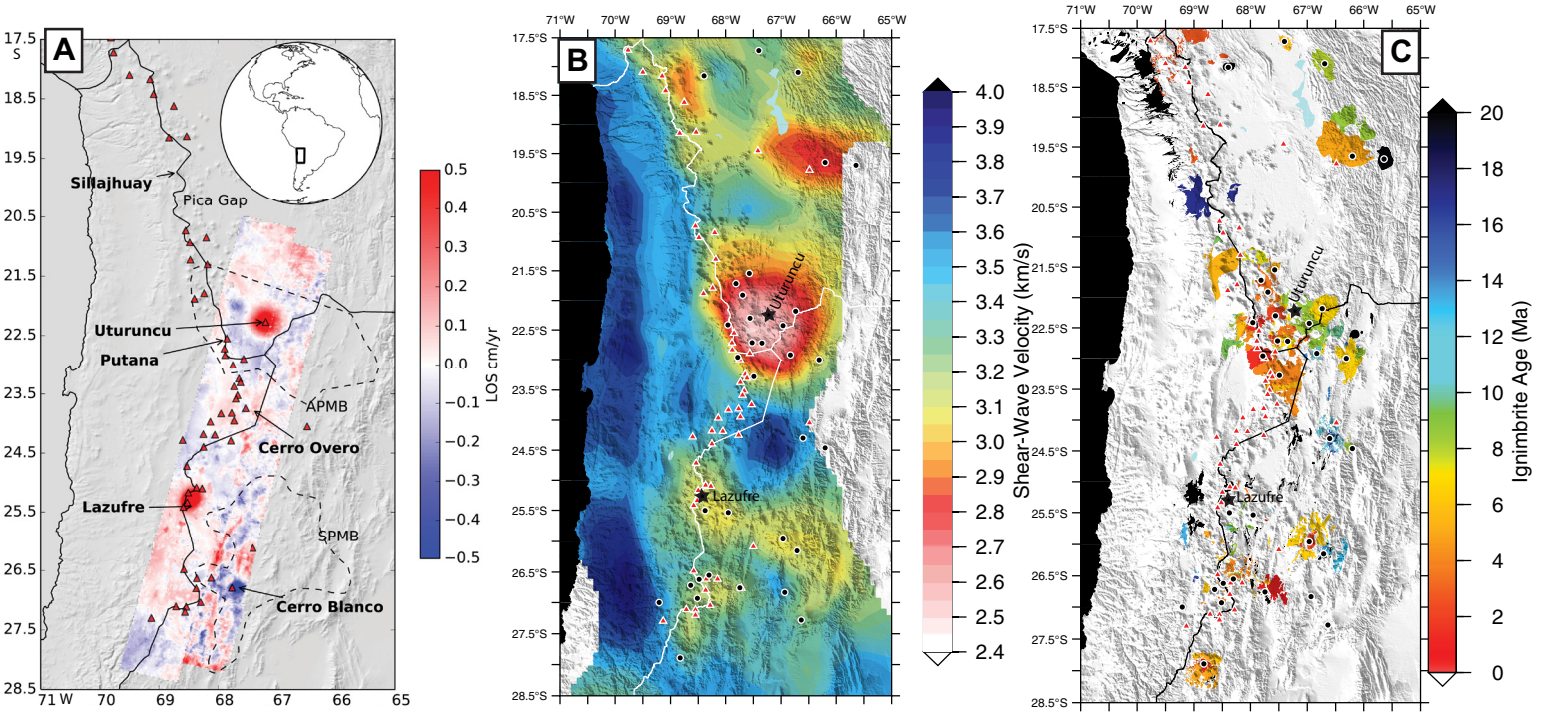

Figure 1. Regional context for the PLUTONS project. (A) Ground deformation between 1992 and 2011 observed by satellite interferometric synthetic aperture radar (InSAR) (from Henderson and Pritchard, 2013) shows large-scale uplift at Uturuncu and Lazufre, which are located, respectively, on top of and near the edge of geophysically inferred zones of partial melt (e.g., Altiplano-Puna Magma (or Mush) Body [APMB], Zandt et al., 2003; Southern Puna Magma Body [SPMB], Bianchi et al., 2013). (B) Low seismic Vs velocities centered in the mid-crust (15 km depth) as derived from ambient noise tomography (Ward et al., 2013; Ward et al., 2014a) are often correlated with Neogene calderas (black circles). (C) Location of ignimbrites in the Central Andes from Brandmeier and Wörner (2014, 2016), augmented by Naranjo et al. (2018a). Holocene volcanoes (including those with questionable ages) from the Smithsonian Institution are shown as red triangles, and Uturuncu and Lazufre are shown as labeled black stars in B and C. LOS—line of sight.

Uturuncu is a Pleistocene dacitic volcano located behind the modern volcanic arc that last erupted 250 ka (Muir et al., 2015). It lies above a large region of inferred crustal melt called the APMB (Figs. 1 and 2), which is near an ignimbrite flare-up over the past ten million years that has formed the Altiplano-Puna Volcanic Complex (APVC, Fig. 1) and which is now waning (Table 1). Deformation at Uturuncu is spatially larger than at Lazufre and has a longer duration deformation history (Table 1). Before the start of the PLUTONS project, Uturuncu was the only known Pleistocene volcano in the world that had active fumaroles, was uplifting, and was seismically active (Sparks et al., 2008).

Lazufre (Pritchard and Simons, 2002) is ~10 km from two Pleistocene–Holocene–andesitic-dacitic arc volcanoes (Lastarria and Cordón del Azufre). Hundreds of older (Quaternary) volcanic vents are present within the deforming area (e.g., Froger et al., 2007) with circumferential and radial patterns (Ruch and Walter, 2010; Perkins et al., 2016a). A connection between Lazufre and Lastarria is suspected, because a smaller and shallower uplift began at Lastarria sometime between 2000 and 2003 (e.g., Froger et al., 2007; Ruch et al., 2009), plausibly related to its active hydrothermal system that has produced liquid sulfur flows (Naranjo, 1985, 1988). Deformation at Lazufre induced extension at Lastarria (e.g., Ruch et al., 2009; Nikkhoo et al., 2016).

The two study sites provide different perspectives on magmatic systems from intrusion to eruption within the Central Andes. One site is within the modern frontal volcanic arc (Lazufre), and the other is 70 km east of the modern arc in an area currently underlain by mid-crustal partial melt (Uturuncu). However, the two sites did not receive equal study. Uturuncu was the primary site with more papers in the themed issue than Lazufre. The choice of two sites mitigated against the possibility that one of the sites could cease activity during the project. We found several indications of decadal temporal variabil-

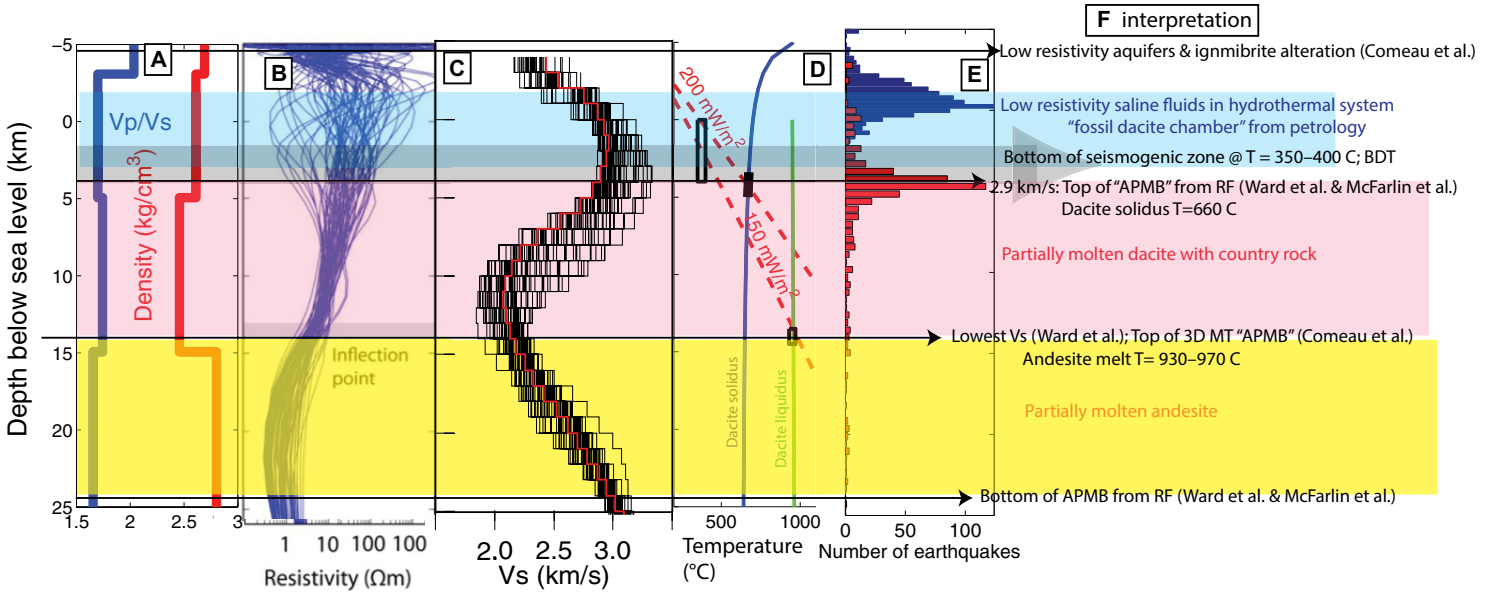

Figure 2. One-dimensional (1D) profiles of features below Uturuncu inferred from geophysics with interpretation consistent with petrology. See Table 2 for further information. (A) Inversion for 1D Vp/Vs and density model below PLUTONS seismic array from receiver functions, Rayleigh wave velocity dispersion from ambient noise and teleseismic earthquakes, and Rayleigh wave H/V ratios from earthquakes (Shen et al., 2017). (B) The preferred 3D magnetotelluric (MT) inversion model (Comeau et al., 2016) plotted as depth-resistivity profiles beneath all 96 MT stations. The inflection point of the resistivity-depth profile is at 13–14 km below sea level (bsl), interpreted as the top of the low-resistivity zone C2 (Figs. 3 and 4). (C) The S-wave velocity model of Ward et al. (2014b) from a joint inversion of ambient-noise tomography data and receiver functions (ANT+RF) is shown below Uturuncu. The red line is directly below the summit (–67.2°W, –22.3°S) and the black lines are from 0.3° to the EW and NS every 0.1° (or ~75 km across in either direction, about the size of the uplifting area). Velocity < 2.9 km/s is inferred to include partial melt (Ward et al., 2014b). The slowest seismic velocities align with the MT-derived inflection point. (D) Subsurface inferred temperatures (see panel F) compared with the dacite solidus (Holtz et al., 2005) and liquidus (Muir et al., 2014a) and calculated geotherms for different values of heat flow using Equation 4 from Chapman (1986), assuming thermal conductivity of 2.7 W/mK (Arndt et al., 1997) and the value of radioactivity in the upper crust from McKenzie et al., (2005) (the heat production in the crust of the Central Andes is considered average: Lucassen et al., 2001). The two lines bracket the geotherm of de Silva and Gosnold (2007) but are both higher than the geotherms of Babeyko et al. (2002) and Fialko and Pearse (2012). (E) Earthquake depths within the seismic network, with more than ten phase picks, between the years 2009–2010 in blue (Jay et al., 2012) and from 2010 to 2012 in red (Kukarina et al., 2017). (F) Interpretation of features in plots A–E, aided by compositional measurements (e.g., Muir et al., 2014b). APMB—Altiplano-Puna Magma (or Mush) Body; BDT—Brittle Ductile Transition.

TABLE 1. SUMMARY COMPARISON OF DIFFERENT OBSERVATIONS OF THE UTURUNCU AND LAZUFRE MAGMATIC SYSTEMS

Characteristic	Uturuncu	Lazufre
Ignimbrites within 150 km (approximately the extent of the low-velocity anomaly, Fig. 1B)	Waning number of large eruptions over past ten m.y.; three major ignimbrite eruptions within 60 km in past two m.y. (Laguna Colorado, 60 km^3 at 1.98 Ma, Puripica Chico, 10 km^3 at 1.7 Ma, Purico ~100 km^3 at 1 Ma)[1]	Waxing ignimbrite activity at Cerro Galán (150 km away) over past six m.y. (2000 km^3 at 2.2 Ma^2). Within 60 km: Caletones Cori ignimbrite ~1.37 km^3 at 0.46 Ma,[3] 185 km^3 Los Colorados ignimbrite ca. 9 Ma[4] (Fig. 1C)
Geomorphology	No net uplift associated with current uplift, implies uplift and subsidence cancel over ~16,000 years[5]	No net uplift in past 16,000 years, but 500 km topographic swell that is older than 0.4 Ma[5]
Decadal ground deformation	Uplift and moat of subsidence ongoing for ~50 years,[6] but the rate is variable[7]	Uplift without a moat of subsidence; began in 1997–1998; the rate of uplift increased and decreased[8]
Hydrothermal system geophysical activity	Hydrothermal system not deforming before 2014 but earthquakes[9]	Hydrothermal system at Lastarria uplifting[10] with earthquakes[11]
Temperature and gas emissions from fumaroles at surface	Low-temperature fumaroles over large area,[12] implies magma is deep	"Magmatic" fumarole temperatures,[13] implies magma is shallow or well connected to the surface
Composition, age, and type of erupted products	Exclusively effusive dacitic eruptions between 0.3–1.1 Ma[14]	Lastarria: 0.5–0.1 Ma, effusive and explosive[15] Cordón del Azufre: 0.6–0.3 Ma, lava and pyroclastic flows, domes.[16] Both: andesites-dacites[17]
Seismicity below hydrothermal system	Maximum depth of earthquakes 6–9 km below surface (Fig. 2), implies temperature of 350–400 °C at those depths	Earthquakes up to 10 km deep[18]
Inferred subsurface melt depth and degree of melting	Region with large volume of melt (APMB): ~500,000 km^3 4–24 km below surface with ~20%–30% partial melt.[19] Evidence for melt extending to the lower crust[20]	In region of mid-crustal partial melt (10–20 km depth, 5%–8% melt)[21]: shallow melt (0.4–6 km below surface 25%–30% melt)[22]

References: [1]Kern et al., 2016; [2]Francis et al., 1983; [3]Richards and Villeneuve, 2002; [4]Naranjo et al., 2018a; [5]Perkins et al., 2016a; [6]Gottsmann et al., 2018; [7]Henderson and Pritchard, 2017; [8]Henderson et al., 2017; [9]Jay et al., 2012; Alvizuri and Tape, 2016; [10]Froger et al., 2007; Ruch et al., 2009; [11]Spica et al., 2012, 2015; [12]Jay et al., 2013; [13]Aguilera et al., 2012; [14]Muir et al., 2015; [15]Naranjo and Cornejo, 1992; Naranjo, 2010; Naranjo et al., 2013; [16]Naranjo et al., 2018b; [17]Wilder, 2015; [18]preliminary: Heather McFarlin, 2017, personal commun.; [19]Ward et al., 2014b; [20]Kukarina et al., 2017; [21]Budach et al., 2013; Delph et al., 2017; Ward et al., 2017; [22]Spica et al., 2015; Díaz et al., 2015. APMB—Altiplano-Puna Magma (or Mush) Body.

ity at the two sites (Henderson and Pritchard, 2017; Henderson et al., 2017). We compare the characteristics and possible interpretations of the two sites in the Discussion section and Table 1.

The PLUTONS project began in 2009 with funding from the UK National Environmental Research Council (NERC) for four years (focused solely on Uturuncu) and the U.S. National Science Foundation (NSF) Continental Dynamics program for five years. The name PLUTONS is a shortened acronym from the names of the magmatic systems and the funding and partner agencies: Probing Lazufre and Uturuncu TOgether: Nsf (USA), Nerc (UK), Nserc (Canada), Sergeotecmin (Bolivia), Sernageomin (Chile), Sernap (Bolivia), observatorio San Calixto (Bolivia), Chilean Seismological service, Universidad de Salta (Argentina).

This themed volume summarizes the key results of the PLUTONS project with the following objectives:

(1) quantify the rates of intrusion and eruption at Lazufre, Uturuncu, and nearby centers, and determine whether those rates have been steady or episodic over the past several million years;
(2) identify and characterize active intrusions, including their depth, volume, temperature, melt content, and shape and how they relate to magma chambers; and
(3) constrain how the active intrusions interact with their surroundings through deformation, faulting, associated fluid flow, metamorphic reactions, and geothermal activity.

PREVIOUS WORK

The PLUTONS project builds on previous regional geochemical, geological, and geophysical studies in the Central Andes. Several previous publications summarize the magmatic evolution of this region in the past ~25 m.y. (e.g., Hawkesworth et al., 1982; de Silva, 1989; Coira et al., 1993; Ort et al., 1996; Lindsay et al., 2001; Schmitt et al., 2001; de Silva et al., 2006; Kay and Coira, 2009; Folkes et al., 2013; Burns et al., 2015; Freymuth et al., 2015) and the geophysical characteristics of the subsurface (e.g., Schmitz et al., 1997; Chmielowski et al., 1999; Schilling et al., 2006; Beck et al., 2015; Pritchard and Gregg, 2016). We

note a few key points here for context. In the Central Andes, volcanic activity has taken place from the volcanic arc to hundreds of km east in the backarc, including large-volume ignimbrites (Fig. 1C), as well as other centers of mostly silicic effusive and explosive magmatism with subsidiary mafic centers (e.g., de Silva and Francis, 1991; Kay and Coira, 2009). The timing, location, and type of activity have varied along strike, but two important regions have been identified (e.g., Kay and Coira, 2009; Beck et al., 2015):

1. Between ~21° and 24° S, an ignimbrite province (>15,000 km^3 erupted) between 11 and 1 Ma called the APVC (de Silva, 1989) surrounds Uturuncu (Fig. 1C). The onset of volcanism in the APVC has been correlated with marked steepening of the subducting Nazca plate from nearly flat-slab subduction prior to 16 Ma to subduction with a ~30° dip today (e.g., Barazangi and Isacks, 1976; Allmendinger et al., 1997). The onset of steepening is thought to have induced decompression and dehydration melting in the mantle and may have facilitated delamination of the base of the continental lithosphere (e.g., Allmendinger et al., 1997; Kay and Coira, 2009). Below the APVC is a large volume (~200 km in diameter) of inferred partial melt, called the Altiplano-Puna Magma (or Mush) Body (APMB), which has been identified by seismic (e.g., Chmielowski et al., 1999; Zandt et al., 2003), gravity (Prezzi et al., 2009), and electromagnetic methods (e.g., Brasse et al., 2002; Schilling et al., 2006).
2. A region between 24° and 28° S that includes the large-volume backarc Cerro Galán ignimbrites (6–2 Ma), numerous, smaller centers, and the volcanic arc that includes Lazufre (Fig. 1C). The zone of partial melt below Cerro Galán, extending to Lazufre and other areas has been called the Southern Puna Magma Body (SPMB, Fig. 1A) (e.g., Bianchi et al., 2013. Several smaller features include the Lazufre Magma Body (LMB) and Cerro Galán Magma Body (CGMB) (Delph et al., 2017; Ward et al., 2017), but the seismic velocity reduction in the mid-crust (Fig. 1B) and the inferred amount of partial melt are less than in the APMB.

One proposed explanation (e.g., Beck et al., 2015) for the older age of ignimbrite volcanism and larger inferred amount of crustal melt in the APMB compared to the SPMB is that slab-steepening and subsequent lithospheric delamination that are driving volcanism are older in the APMB than in the SPMB. Additional factors are N-S variations in crustal thickening, tectonic variations in the upper plate, and oblique subduction of the Juan de Fuca Ridge (e.g., Kay and Coira, 2009; Freymuth et al., 2015; Brandmeier and Wörner, 2016; Naranjo et al., 2018a, 2018b).

DATA COLLECTION

Figure 3 shows a map of the geophysical networks deployed by the PLUTONS project, and in the Appendix, we summarize new geochemical and geophysical data and how they were analyzed. Results of these studies and numerical modeling are described in the subsequent sections.

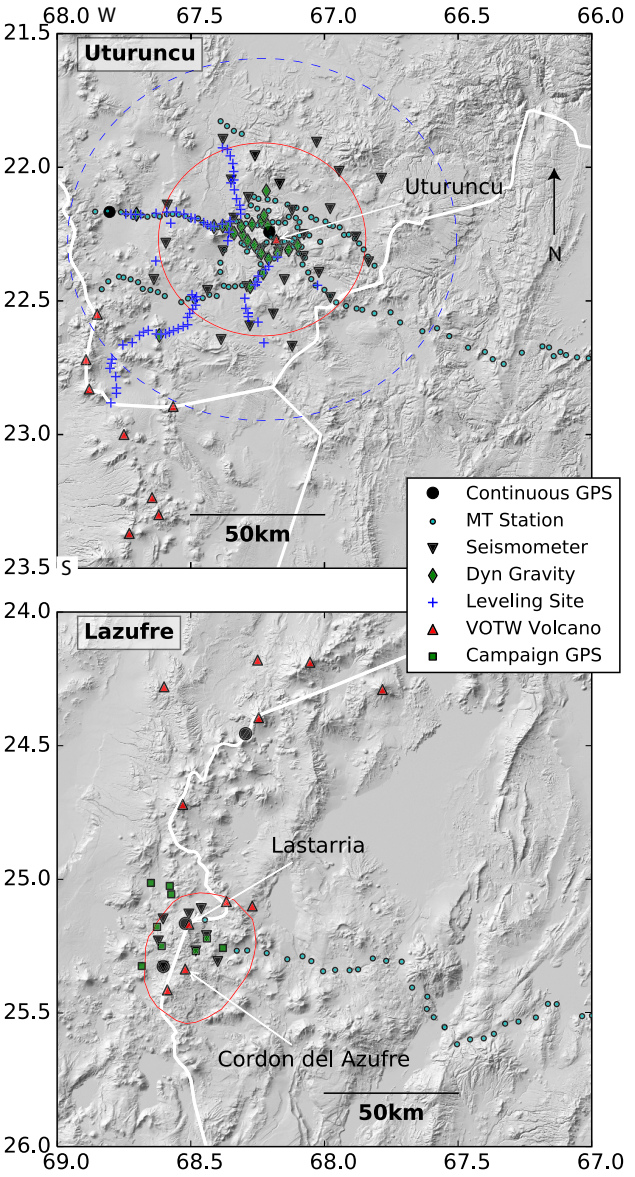

Figure 3. PLUTONS geophysical instruments deployed at Uturuncu (top) and Lazufre (bottom). Approximate outlines of uplifting regions are shown by the red contour (between 1992 and 2011 for Uturuncu from Henderson and Pritchard, 2013; 2006–2008 for Lazufre from Remy et al., 2014) and subsiding region at Uturuncu is inside the dotted blue line. Holocene volcanoes from the Smithsonian Volcanoes of the World catalog are shown as red triangles. See text for description and references for each geophysical technique.

RESULTS

Below we summarize key results of the PLUTONS project and other recent projects in the region in the context of previous work. We describe the results from individual studies of Uturuncu and Lazufre and synthesize them into estimates of the amount of partial melt as a function of depth. Because the regional altitudes near Uturuncu and Lazufre are 5 and 4.3 km above sea level, respectively, we label all depths as either beneath these locally defined surfaces or below sea level (bsl).

What Did We Learn About Uturuncu and the APMB?

Seismic Velocities as a Function of Depth

The thickness of the APMB seismic anomaly using newly available data and analyses through ambient noise tomography and receiver functions is on average 9–11 km (Ward et al., 2014b, 2017; McFarlin et al., 2018), as opposed to ~1–2 km estimated in previous work (e.g., Leidig and Zandt, 2003). The dimensions of the APMB can be defined by the 2.9 km/s Vs velocity contour, because velocities below this value likely require fluids (such as melt or brines) and are difficult to explain by anisotropy or temperature variations alone (Ward et al., 2014b). Below Uturuncu, the Vs = 2.9 km/s contour is as shallow as 4 km bsl with a minimum velocity and a presumed highest melt fraction at 10–15 km bsl (Fig. 2C). PLUTONS seismic data show lateral and vertical variations in the low-velocity zone not imaged in previous work (e.g., Yuan et al., 2000), with lower Vs (<2.0 km/s) as well as varying thickness (5–20 km) and depth (9–19 km) below the surface (Ward et al., 2014b, 2017; McFarlin et al., 2018).

A different view of seismic velocities is provided by earthquake tomography. Kukarina et al. (2017) image a vertical structure 20–30 km wide below Uturuncu; this structure extends from ~6 km below the surface into the lower crust with low Vs (Fig. 4E) and Vp/Vs >1.9 (Fig. 5A). The bottom is not well resolved because of vertical smearing of the tomography. The APMB is largely invisible to Vs earthquake tomography because the local seismicity lies mostly above it (Jay et al., 2012; Kukarina et al., 2017), while the subducting slab seismicity cannot resolve uniform layers of low velocity that extend across the entire network (Kukarina et al., 2017). The ambient noise tomography and receiver functions analysis of Ward et al. (2014b) could not resolve this vertical feature very well because it is smaller than the spatial resolution of the long-wavelength surface waves used in that study (30–100 km). However, a vertical anomaly below Uturuncu is just visible at depths greater than 20 km bsl (Fig. 4D) in the analysis of Ward et al. (2017). The Vp earthquake tomography image (Fig. 4F) is quite different from the Vs image (Fig. 4E); there is a regional low Vp at the depth of the APMB, but there is a Vp high directly below Uturuncu at 10 km depth.

Receiver functions show topography on the top of the APMB and a velocity change in the lower crust that varies laterally. Specifically, there is a change in the depth of a sharp velocity contrast from 60 km regionally (possibly the Moho) to 40 km below Uturuncu (Fig. 5) (McFarlin et al., 2018). The 40 km reflector is not the Moho since the seismic velocities below it are not mantle velocities (Ward et al., 2017), but the reflector could indicate the top of a localized mafic lower crust, possibly formed as a plexus of mafic and/or ultramafic sills or cumulates due to basaltic magma intrusion (e.g., Müntener and Ulmer, 2006; Nandedkar et al., 2014). A high Vp anomaly in the lower crust below Mount St. Helens has been explained by ultramafic cumulates (Kiser et al., 2016) and is similar in spatial scale to the observations at Uturuncu. A Vp anomaly is not detected in the lower crust of Figure 4F but would be hard to resolve (Kukarina et al., 2017).

Subsurface Electrical Resistivity

Previous work revealed a large low-resistivity subsurface zone around Uturuncu (e.g., Schilling et al., 2006), but the improved data and methods used by Comeau et al. (2015, 2016) reveal several resistive anomalies in the upper crust that may be connected with the APMB and surface volcanic features (Figs. 3B, 3C, 4B, 6B). The largest region with the lowest resistivity (C2 in Figs. 3B, 3C, and 4) is inferred to be the top of the APMB and is 5 km shallower in the 3D inversion (13–14 km bsl; Figs. 3C and 6B) than the 2D inversion (18–19 km bsl; Fig. 4B). The depth from the 3D inversion (~13–14 km bsl) is identified by the inflection point in 1D resistivity profiles (Fig. 2B) based on synthetic resolution studies (Comeau et al., 2016). Thus the top of the APMB differs by almost 10 km from that of the joint ambient noise tomography and receiver function solution (4–5 km bsl; Ward et al., 2014b). There is a similar difference between the depth to the minimum Vs and lowest resistivity (Fig. 2) (Comeau et al., 2015). This difference is attributed to the different sensitivities of these methods to partial melt of different compositions (discussed in the next section and Fig. 2; Table 2; Comeau et al., 2016; Pritchard and Gregg, 2016).

Gravity and Subsurface Density

A low isostatic and Bouguer gravity anomaly over the APMB (e.g., Götze et al., 1994; Prezzi et al., 2009) and a dense grid of observations used to generate new models have produced a range of plausible subsurface density structures (del Potro et al., 2013). These models show low-density structures connecting the APMB to the surface (dotted lines in Fig. 4B). These structures overlap the MT anomalies.

"Fossil Dacite Magma Chamber" and Hydrothermal System

The volcanic evolution of Uturuncu was summarized by Sparks et al. (2008), Michelfelder et al. (2014), and Muir et al. (2015), with additional geochemical, geochronological, and petrologic data from Michelfelder et al. (2013) and Muir et al. (2014a, 2014b). Volcanic rocks from the edifice of Uturuncu are dominantly crystal-rich, high-K, calc-alkaline, dacite lava flows and domes with phenocrysts of plagioclase > orthopyroxene > biotite > quartz. Groundmass

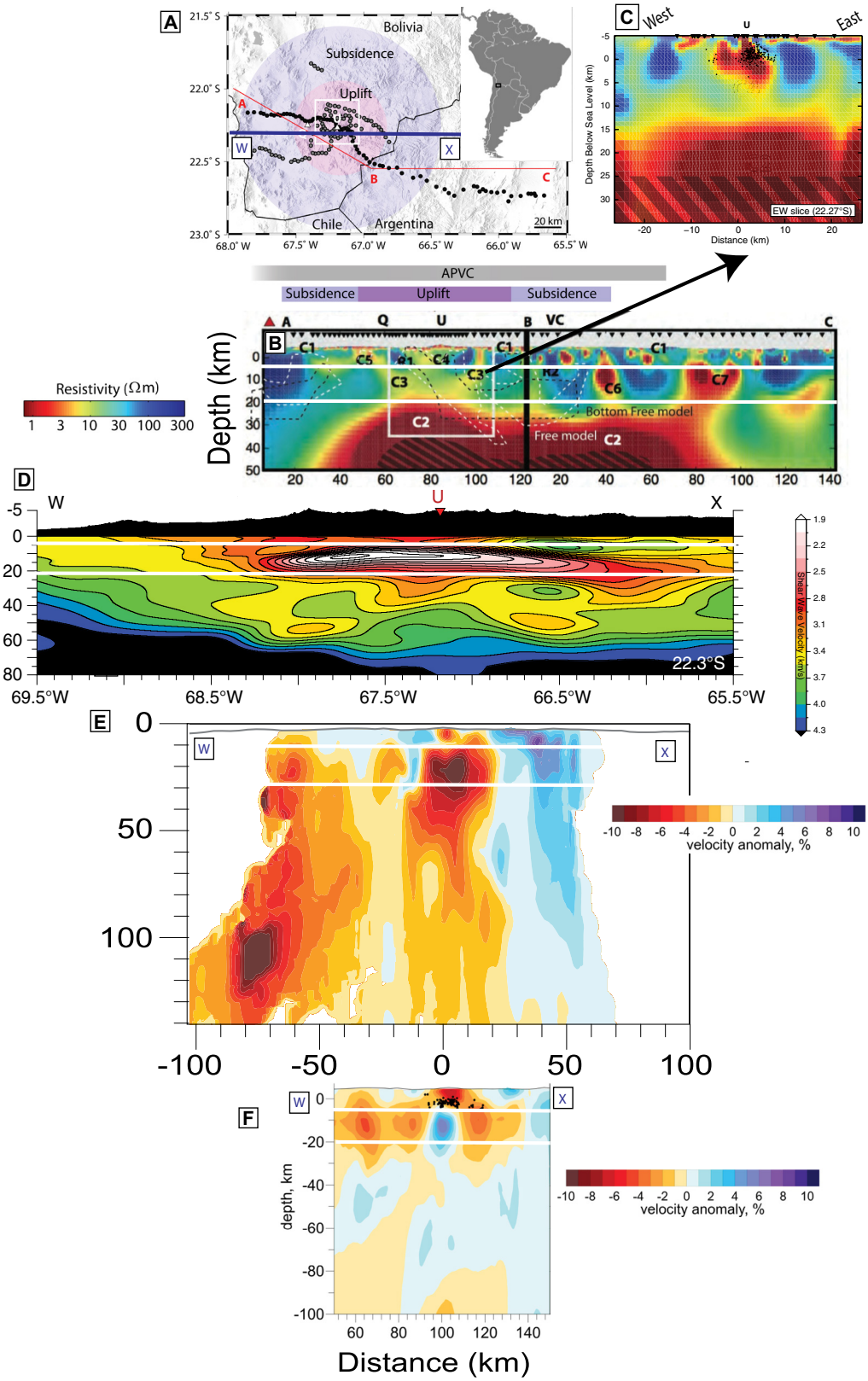

Figure 4. Selected inversion results from geophysical studies of the Altiplano-Puna Magma Body (APMB) near Uturuncu volcano, Bolivia (labeled U). (A) Location map with two shaded rings showing the approximate locations of ground uplift and subsidence around Uturuncu (e.g., Henderson and Pritchard 2013). Black and gray symbols are magnetotelluric (MT) stations used in the inversions in B and C. The red line is the MT profile A-B-C shown in B. The blue line shows the seismic velocity profile shows the seismic tomography profile W-X in D, E, and F. East-west profiles in B, D, E, and F, have been approximately aligned horizontally. (B) Two-dimensional MT inversion along the A-B-C transect shown in A. Low resistivity values (red to yellow) indicate interconnected, electrically conductive fluids, such as brines or partial melt. Dotted lines show regions of low density from two inversions of the gravity data (del Potro et al., 2013). The white-boxed region was investigated with the 3D inversion and is shown by the arrow in C. The model does not resolve the black diagonally hatched areas. Red triangle shows location of volcanic arc, after Comeau et al. (2015), in B. The horizontal white lines in B-F show the approximate locations of the upper and lower Vs = 2.9 km/s contours in d. (C) 3D inversion of region shown in B with same color scale, after Comeau et al. (2016). The low-resistivity region labeled C4 overlaps earthquakes (black dots: Jay et al., 2012) and petrological depth inferences for the dacites (e.g., Muir et al., 2014a, 2014b). Note the change in depth of the upper boundary of the feature C2 between B and C. (D) Vs from joint inversion of seismic ambient noise tomography and receiver functions along the W-X transect shown in A. The large horizontal low velocity zone is the APMB, after Ward et al. (2017). (E and F) Vs and Vp from tomography (same color bar) using earthquakes from the subducting Nazca slab. The low Vs and high Vp below Uturuncu is well resolved in the center of the PLUTONS array, while the low Vs zone in the volcanic arc at the edge of the array is less well resolved (Kukarina et al., 2017). The Vp/Vs ratio from this same profile is shown in Figure 5.

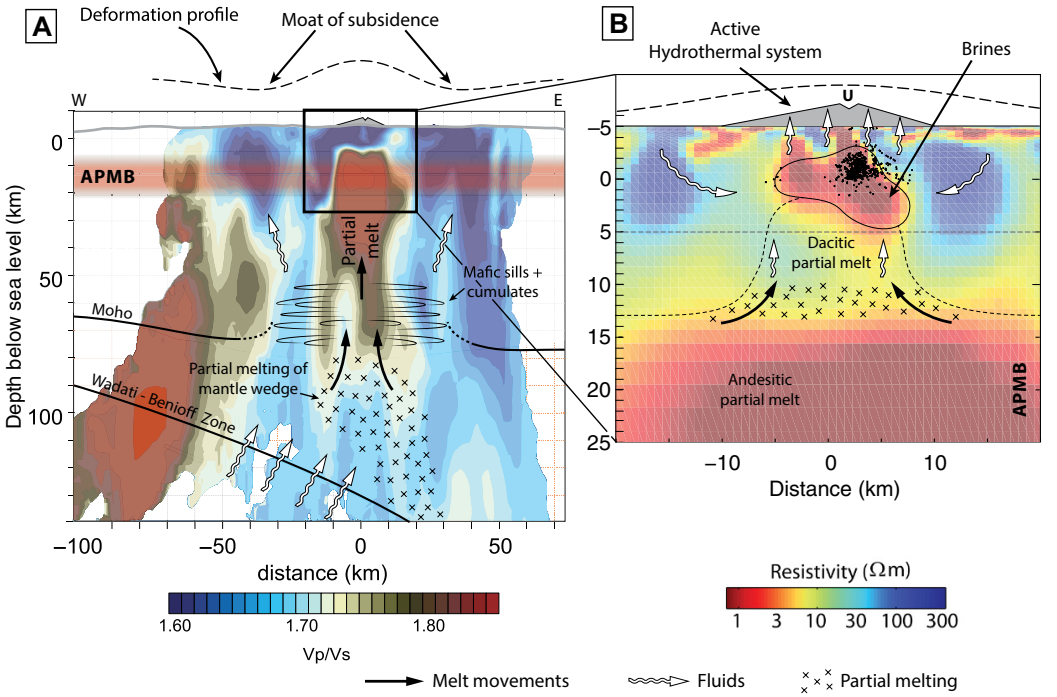

Figure 5. Interpreted cross section at Uturuncu overlain onto geophysical images. (A) The background color shows an EW cross section of inverted Vp/Vs from earthquake tomography (Kukarina et al., 2017: see Fig. 4 for profile location), with other interpreted features labeled; upper surface of subducting slab (Wadati-Benioff Zone) defined by earthquakes; deep crustal reflector (e.g., mafic sills and cumulates) as located from receiver functions from McFarlin et al. (2018); the Altiplano-Puna Magma (or Mush) Body (APMB) from Ward et al. (2014b); and ground deformation from Henderson and Pritchard (2013). Notice the two zones of high Vp/Vs: One region below Uturuncu is well resolved to be ~20 km wide, elongate in the east-west axis; with Vp/Vs ratio >1.9; shallows to 5 km below sea level (bsl); extends deep beneath the APBM. The second region is at the western edge of the model, between 60 and 140 km depth, Vp/Vs is not well resolved, although high Vp/Vs shallower than 60 km on this western edge may be related to the volcanic arc. (B) Cross section of the preferred 3D resistivity model (Fig. 4C) with the deep low-resistivity region interpreted as the APMB and the shallow low resistivity zone interpreted as the hydrothermal system (see text), modified from Comeau et al., 2016. The point labeled U is the location of Volcán Uturuncu. The dotted line shows the region of fluid and/or magma pressurization and depressurization that matches the surface uplift and subsidence (Gottsmann et al., 2017). Black dots are earthquake hypocenters from Jay et al. (2012). The inferred flows of silicate melt and aqueous fluids in the mantle (A) and crust (B) are indicated by arrows. Regions of partial melting within the mantle (A) and within the crust atop the APMB (B) are shown with crosses. Images created by Simon Powell, University of Bristol.

minerals and glass make up 70%–50% of the modal volume. Eruptive activity at Uturuncu was episodic with six eruptive periods separated by >50 k.y. hiatuses with major edifice construction occurring between 595 and 505 ka (Muir et al., 2015).

Petrological analysis (experiments and melt inclusions) suggests that the dacite lavas that erupted at Uturuncu >250 ka were stored 2–4.5 km below the surface (at or above sea level, Muir et al., 2014a, 2014b). There are geophysical anomalies (Table 2: low resistivity, earthquakes, and low Vs; Figs. 3C and 4; e.g., Jay et al., 2012) at approximately the same depth region today. While a shallow dacite magma chamber fed Uturuncu eruptions, it is unlikely that magma is present at shallow depth today. In order to explain the observed resistivities, 80%–100% dacite partial melt would be required (Fig. 6C) because dacitic melt is resistive (e.g., Laumonier et al., 2015; Comeau et al., 2015, 2016). This amount of melt at these depths is implausible—being ruled out by the nonzero values of Vs (e.g., Jay et al., 2012; Kukarina et al., 2017). Instead, the low resistivity of C4 (Fig. 6B) can be explained by saline fluids of magmatic and/or meteoric origin (Comeau et al., 2015, 2016). The resistivity of brines at 300–500 °C (Fig. 2) is 0.1–0.01 Ωm (e.g., Unsworth and Rondenay, 2013), which is consistent with the observed bulk resistivity for plausible values of porosity and fluid interconnectivities (Fig. 6D). For example, if we assume salinity to be 30,000 ppm (3%) and temperature 200–400 °C, the brine resistivity is calculated to be ~0.03 Ωm (Ussher et al., 2000). For plausible upper-crustal interconnected porosity of 5%, we calculate the bulk resistivity observed in the MT-derived model (5 Ωm) using a modification of Archie's Law (Fig. 6D).

The proposed NaCl content is realistic given the composition of Uturuncu dacites, phase relations in the system NaCl-H_2O, and the NaCl contents (10%–50%) measured at other volcanoes (e.g., Aguilera et al., 2016). The dacite magma prior to eruption, as shown by melt inclusions (Muir et al., 2015), contained ≤3.9 wt% H_2O and 0.23 wt% chlorine. If we convert this composition into a bulk equivalent salinity ($NaCl_{eq}$, i.e., assuming all Cl is complexed by cations such as K, Na, and Ca), we calculate 9 wt% or 2.7 mol%. At a solidus temperature of ~600 °C, such a fluid will be supercritical at pressure above 90 MPa but condense to a mixture of high-salinity brine and low-salinity vapor at lower pressures (Driesner and Heinrich, 2007). The corresponding depth depends on the density of the surrounding rock and the extent to which the fluids are interconnected, i.e., lithostatic or hydrostatic pressure. In the former case, with a rock density of 2600 kg/m³ (Fig. 2A), 90 MPa corresponds to 3.5 km depth. In the latter case, taking fluid density as 1300 kg/m³, the depth is 7 km. Thus as magmatic fluids ascend and separate in the depth range 3.5–7 km, brines with compositions consistent with the low-resistivity anomaly are formed (Fig. 6B). Numerical modeling of fluid release and brine condensation above solidifying plutons (Weis, 2015) indicates that the brine can accumulate in cylindrical

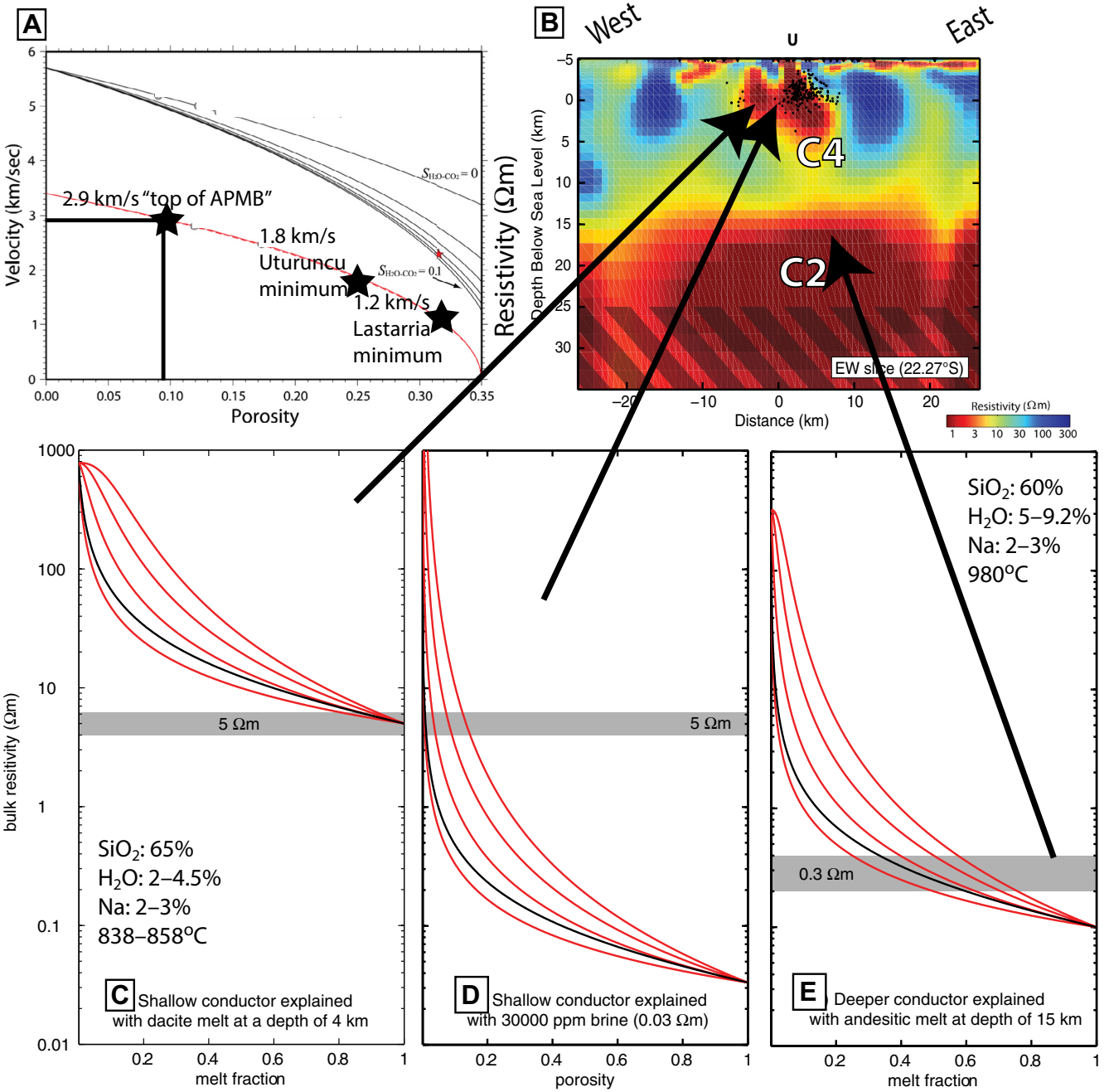

Figure 6. Geophysical inferences of the amount of subsurface melt and/or fluid. (A) Conversion of Vp and Vs to porosity (partial melt plus volatile phase) from Chu et al. (2010). The plot shows the Vs values that were used to define the limits of "significant partial melt" (2.9 km/s, ~10% partial melt, Ward et al., 2014b), the minimum Vs seen beneath Uturuncu in the Altiplano-Puna Magma (or Mush) Body (APMB) (1.8 km/s, implying 25% partial melt) and beneath Lastarria volcano (1.2 km/s, implying ~32% porosity) near the Lazufre deformation center. (B) The 3D resistivity model from Comeau et al. (2016) and (C–E) show variation of bulk resistivity as a function of the quantity of fluid all at Uturuncu. (C) Model predictions of bulk resistivity of the shallow low-resistivity region from dacite melt using the chemical composition of the melt (Comeau et al., 2015). The gray bar shows the observed value from the model in (B) which can only match the models at unrealistically high melt fraction. (D) Model prediction of bulk resistivity from the same region as (C) from a mix of aqueous fluids and dacite. A porosity <5% of interconnected salty aqueous fluids is needed to explain the observed resistivity. (E) Bulk resistivity of the deeper low-resistivity feature modeled with andesite melt having resistivity of 0.1 Ωm (Comeau et al., 2015). In C, D, and E, the red curves use a modified Archie's Law with cementation exponents of 1, 1.5, 2, and 2.5. The black curve shows the Hashin-Shtrikman upper bound, and represents well-interconnected fluids.

TABLE 2. INTERPRETATION OF DIFFERENT PARAMETERS BENEATH UTURUNCU ALSO SHOWN IN FIGURE 6

Depth	Observations	Interpretation
0 to 1 km: Near surface	Surface temperature at fumaroles: 80 °C (Sunagua, 2004; Sparks et al., 2008; J. Gottsmann, 2011, personal commun.; boiling temperature at this altitude), but air temp average probably close to 0 °C based on Uyuni weather station, which is at lower elevation. Heat flow: nearest measurements are tens to hundreds of km away, 55–150 mW/m^2–100–200 mW/m^2 used in BDT calculations (summarized in Jay et al., 2012). Magnetotellurics (MT) shows spatially variable low resistivity layers <1 km.	Consider 150–200 mW/m^2 as viable range given other constraints (Fig. 2D). Low resistivity related to hydrothermal alteration of the ignimbrites (Comeau et al., 2015) and shallow aquifers (Comeau et al., 2016).
2–4.5 km below surface: "fossil dacite chamber" and hydrothermal system	From experiments and melt inclusions, erupted dacites sourced from 50–119 MPa (Muir et al., 2014a, 2014b). MT shows three E-W trending low-resistivity anomalies (~1 Ωm, Fig. 2B), Shallow ambient noise shows low Vs (minimum ~2.5 km/s) 1.9–3.9 km below surface (Jay et al., 2012), oriented NS (i.e., in contrast with the MT anomalies)—maybe they have different causes? Earthquake tomography shows a low Vs and high Vp/Vs anomaly here, but there is a question of whether the low Vs region is resolved at this shallow level (Kukarina et al., 2017). Shallow earthquakes in this region (Jay et al., 2012).	With a density of 2700 kg/m^3, dacite magma chamber is 2–4.5 km below surface. Infer 702–925 °C at this depth episodically between ca. 250–1000 ka (Muir et al., 2014a, 2015). Implies heat flow would be >400 mW/m^2 if in equilibrium then, but is lower today. Not likely to be melt here today, but a spatially heterogeneous mixture of high-resistivity dacite, low-resistivity aqueous fluids, and low-resistivity, hydrothermally altered dacite (Comeau et al., 2015, 2016).
5–9 km below surface: bottom of seismogenic zone (350–400 °C), BDT	Earthquakes mostly above ~5 km depth (Fig. 2E) from Jay et al. (2012), but Hutchinson (2015) and Kukarina et al. (2017) put maximum depths at ~9 km using different seismic velocity models with focal mechanisms constrained by Alvizuri and Tape (2016). MT values in this depth range ~3 Ωm (Comeau et al., 2016).	Bottom of the seismogenic zone 5–9 km, interpreted to be between 350 °C (McKenzie et al., 2005) and 400 °C (Smith et al., 2009) in Figure 2D. This depth to seismogenic zone bottom overlaps the range calculated for the brittle-ductile transition (Jay et al., 2012). Resistivity increases with depth permeability decreases for brines.
9 km below surface: "Top" of APMB (from Ward et al., 2014b), dacite partial melt, T = 660 °C	Below Uturuncu, this depth is where Vs <2.9 km/s and is a depth that shows up as a strong velocity gradient in the receiver functions (McFarlin et al., 2018). At 6 km below the surface, the Vp/Vs ratio changes from ~1.6 to >1.9 based on earthquake tomography (Kukarina et al., 2017), but at 10 km below the surface, Shen et al. (2017) have their 1D model Vp/Vs increase from 1.65 to 1.79, corresponding to a density decrease from 2590 to 2460 kg/m^3. The MT shows no distinct feature at this depth, although this is near the bottom of the 3 Ωm "fossil dacite chamber" seen at shallower depths, and the resistivity increases to nearly 10 Ωm (Comeau et al., 2016).	Vs <2.9 km/s requires significant partial melt (Ward et al., 2014b, Fig. 2C). If at the dacite solidus at this depth, T = 660 °C (Holtz et al, 2005) implies ~200 mW/m^2 and 83 K/km if in thermal equilibrium (consistent with a seismogenic zone bottom ~5 km depth, Fig. 2D). Shear velocity is quite insensitive to the composition of the melt (Dvorkin, 2008), and a layer with 15%–25% melt is calculated to match the seismic velocities (Comeau et al., 2016). The higher resistivity could be related to fewer brines because of reduced porosity with increasing depth (e.g., Kuang and Jiao, 2014) and/or disassociation of smectite causing higher resistivity.
18–19 km below surface "Top" of APMB (Comeau et al., 2015), andesite partial melt, T = 930–970 °C	MT inflection point, signifying the top of the low-resistivity zone C2 (Fig. 2B). At about this depth, the density increases and the Vp/Vs decreases (Shen et al., 2017; Fig. 2A), but this is not seen by Kukarina et al. (2017); instead they see a high Vp and low Vs (giving Vp/Vs >2). The lowest Vs (~1.8 km/s) from Ward et al. (2014b) are at ~18 km depth below Uturuncu surface with MT minimum at 0.3 Ωm (Comeau et al., 2016).	Andesite partial melt with 9 wt% H_2O, T = 930–980 °C (Muir, 2013). These temperatures imply heat flow of ~150 mW/m^2 and predict the seismogenic zone bottom at ~8 km (consistent with observations) if in thermal equilibrium. This temperature is also about the liquidus temperature for dacite (Fig. 6D). This region shows accumulations of melt-rich zones in the upper part of a transcrustal magma system (see Sparks and Cashman, 2017).
19–70 km deep: Vertical "melt zone" connects APMB and 40 km reflector	ANT/RFs give "bottom" of APMB 24–27 km below surface (Ward et al., 2014b). MT doesn't well resolve bottom (it may not be discrete), but based on conductance, it is at least 6–20 km thick (Comeau et al., 2016), putting the depth 25–39 km below surface.	Higher Vs and velocity gradient at ~40 km detected by receiver functions (McFarlin et al., 2018) may indicate more mafic composition; for example, cumulates.

Abbreviations: ANT/RF—ambient-noise tomography data and receiver functions; APMB—Altiplano-Puna Magma (or Mush) Body; BDT—brittle-ductile transition.

bodies similar in scale to those imaged. For a pluton at 5 km depth exsolving fluids with 10 wt% $NaCl_{eq}$, Weis' (2015) calculations show brine accumulation at 1–5 km depth as shown in Figure 6D.

Inferred Partial Melt

Converting geophysical observables to estimates of the amount of partial melt requires assumptions about the nature of crustal anisotropy (e.g., Ward et al., 2014b), the distribution of melt at the grain scale (i.e., dihedral angle; see Forsyth, 1993) and in veins, dikes, and sills too small to be resolved by geophysical inversions, and the level of melt interconnectivity (e.g., Unsworth and Rondenay, 2013). For example, the calculations shown in Figure 6 assume that melt is interconnected (or not) at the microscale along grain boundaries, but larger-scale melt-rich regions (composed of layers, dikes, sills, veins, etc. spanning meters to km) are considered plausible (e.g., Schmitz et al., 1997; Jackson et al., 2003; Schilling et al., 2006; Solano et al., 2012, 2014; Sparks and Cashman, 2017). They cannot be geophysically resolved as individual features but might be seen in seismic anisotropy if there was a dominant orientation (e.g., Jaxybulatov et al., 2014).

The melt percentage of the APMB is at least 10%–25% based on combining the seismic and MT observations with laboratory-derived relations between Vs, resistivity, attenuation, and melt percentage using appropriate pressure, temperature, and compositional inferences from volcanic samples (e.g., Fig. 6; Schilling et al., 2006; Ward et al., 2014b; Comeau et al., 2015, 2016; Farrell et al.,

2017). Melt volumes up to 80%–90% are permitted by the gravity and MT data (e.g., del Potro et al., 2013; Comeau et al., 2015). But bulk values of partial melt above 35%–50% would produce a Vs "shadow zone" in silicic melts (e.g., Chu et al., 2010)—i.e., no S waves would be recorded at the surface above this zone, which has not been observed (e.g., Schilling et al., 2006).

Temporal Variations in Ground Deformation

A globally anomalous pattern of surface deformation is centered approximately on Uturuncu with a central uplift and surrounding ring of subsidence with a diameter of 150 km that some have called a "sombrero" (e.g., Fialko and Pearse, 2012; Henderson and Pritchard, 2013). The sombrero is superimposed on an ~1-km-high topographic anomaly across the APVC with a wavelength of ~230 km (Perkins et al., 2016b). The deformation seems to have been ongoing from at least 1965–2010 with a maximum uplift rate of 1.2 ± 0.1 cm/yr and subsidence of 0.3 ± 0.03 cm/yr coincident with the interferometric synthetic aperture radar (InSAR) observed uplift and subsidence (Gottsmann et al., 2017). But, the rate is variable—in the 1990s, vertical rates are greater than 0.7 ± 2 cm/yr at GPS station UTUR; rates decrease to 0–0.1 cm/yr in 2010 and then increase to 0.9 cm/yr in 2015 (Henderson and Pritchard, 2017). There is no net geomorphic deformation of river profiles or lake shorelines across the current uplift field at Uturuncu, which implies that the uplift must have been of less than 100 years duration at the average uplift rates from 1992 to 2011 (Perkins et al., 2016a). Any similar episodes of uplift must have been balanced by subsidence to create no net deformation over the past 16,000 years (Perkins et al., 2016a). A model for the distribution of lineaments around Uturuncu is presented by Walter and Motagh (2014) as evidence of subsidence, although the structural interpretation of these features has been questioned by the original authors as well as by Perkins et al. (2016a). Given the wide spatial footprint of the deformation and coupled uplift and/or subsidence, the deformation is likely caused by processes in the middle to lower crust (regional crustal thickness is 60–70 km). Possible processes include an active diapir (e.g., Fialko and Pearse, 2012; del Potro et al., 2013) and the transfer of magma and magmatic fluids from deeper to shallower levels within a large-scale mushy magma system (Fialko and Pearse, 2012; Henderson and Pritchard, 2013, 2017; Gottsmann et al., 2017; Sparks and Cashman, 2017). A mid-crustal source is consistent with the lack of gravity change associated with the deformation (Gottsmann et al., 2017). We discuss the merits and limits of these models in the section on "Conceptual Models for Deformation at Uturuncu and Lazufre."

Synthesis of Uturuncu Observations into a Depth Profile

Here we explore the possibility of making a self-consistent interpretation of all data sets, considering that each one is sensitive to different properties, following the approach of Comeau et al. (2016). Our approach is non-unique and can only be considered semiquantitative because we have not created a unified numerical model that is consistent with all data sets. We put forward this model (Fig. 2; Table 2) with some falsifiable predictions to summarize our current understanding. The key interpretations are at three depths: (1) shallow depths less than 5 km below the surface; (2) between 9 and 18 km depths; and (3) 18 km and below.

(1) At depths 2–4.5 km below surface, the low resistivity (Fig. 4C) and low Vp and Vs (Fig. 4C; Jay et al., 2012; Kukarina et al., 2017) suggest brines in the hydrothermal system (Fig. 5D). As depth increases, the permeability decreases, and so the geophysical expression of these brines decreases.
(2) At ~9 km below the surface, the top of the APMB is defined by Vs <2.9 km/s (presumed to be at the dacite solidus). The partially molten dacite reduces the Vs, but it is relatively dry (3.2 ± 0.7 wt% H_2O; Muir et al., 2014b) with high viscosity. Consequently, the melt phase may not be well connected, and the melt thus does not reduce the resistivity (Fig. 6C). The high Vp at this depth (Fig. 4F; Kukarina et al., 2017) may reflect a mafic contribution.
(3) There is an inflection point in the resistivity depth profile (Fig. 2B; Comeau et al., 2016) ~18–19 km below the surface where the resistivity decreases significantly. This inflection point is interpreted to be the top of the partially molten andesite. This inferred andesitic melt extends possibly to 25–39 km below the surface (Table 2). The low resistivity is explained by the high water content of the andesite (~9 wt% H_2O; Laumonier et al., 2017) and the melt phase being well connected (Fig. 6E).

Our conceptual model implies approximate temperatures at the bottom of the seismogenic zone, at the top of the APMB as defined seismically by Ward et al. (2014b), and at the top of the APMB as defined using magnetotellurics by Comeau et al. (2016). To estimate the present-day surface heat flow, we assume that heat loss is purely by thermal conduction, that the system is in steady state, use the inferred temperatures in Figure 2D and Table 2, along with the equation for heat flow = k*dT/dz (where k is thermal conductivity and dT is the temperature difference between depths dz), to find a heat flow of 150–200 mW/m^2. These values can be tested with future heat-flow observations. We emphasize that the depths shown in Figure 2 and Table 2 correspond to depths below Uturuncu, and we know that these vary spatially at other locations within the APMB.

What Did We Learn About Lazufre?

Seismic and Electrical Resistivity as a Function of Depth

Prior to 2002, the Lazufre magmatic system was not known, and only limited geophysical data had been collected. Yuan et al. (2000) identified a region of potential partial melt from one seismometer near Lazufre. Later work using regional Vp earthquake tomography identified a zone of partial melt in the Puna backarc called the SPMB (e.g., Bianchi et al., 2013). Ambient noise tomography that included PLUTONS seismometers (Fig. 1B; Ward et al., 2013; Delph et al.,

2017; Ward et al., 2017) showed a low Vs zone below Lazufre ~50 km in diameter from ~10–20 km bsl that could be an isolated body or related to the SPMB (e.g., Fig. 1B; Ward et al., 2013; Delph et al., 2017; Ward et al., 2017). Shallower low-velocity zones have been found in the Lastarria-Lazufre magmatic system using seismic networks focused on Lastarria (Fig. 7; Table 3; Spica et al., 2015) using ambient noise tomography. Two of these areas within the upper 6 km beneath Lastarria have minimum Vs 1.25–1.8 km/s (implying >30% melt, Fig. 6A) and are thought to be related to a small magmatic system feeding a hydrothermal reservoir (Fig. 7B; Spica et al., 2015). The locations of these low seismic velocity zones also correspond to low resistivity as measured by MT that could be either brines or partial melts (implying melt >40% for andesite; Fig. 7D) in the upper 7 km below Lastarria (Díaz et al., 2015; Fig. 7C) and below 20 km at Lazufre (Budach et al., 2013).

Temporal Variations in Ground Deformation

Ground uplift at Lazufre occurs on two spatial scales: (1) the broad, ~40-km-diameter deformation from Lazufre that began in 1998, and (2) the smaller pattern at Lastarria volcano that spans a few kilometers and began ~2003 (e.g., Pritchard and Simons, 2002; Froger et al., 2007; Ruch et al., 2009; Fig. 7A). The Lazufre deformation was ongoing in 2016, although the rate of deformation has varied in time from ~1 cm/yr from 1998 to 2003, 3 cm/yr from 2003 to 2010, and ~1.5 cm/yr from 2010 to 2016 (e.g., Ruch et al., 2009; Henderson and Pritchard, 2013; Pearse and Lundgren, 2013; Remy et al., 2014; Henderson et al., 2017). Whether deformation has continued at Lastarria after 2008 is not currently known. Analysis of topography suggests that this is not the first episode of uplift at Lazufre because the deformation pattern is coincident with a 500-m-high topographic swell (Froger et al., 2007), implying a source characterized by inelastic deformation. To assess the age of this swell, Perkins et al. (2016a) measured the orientation of lava flows of different ages in the area and concluded that lava flows older than ca. 0.4 Ma were not affected by the presence of the swell—thus, the swell must be younger than 0.4 Ma. The swell formation is thought to be older than ~16,000 years, since the lake shorelines near Lastarria are not tilted (Perkins et al., 2016a). Thus the current uplift is very short-lived, or multiple uplift episodes are counterbalanced by subsidence to produce no net deformation. The implications of this are further explored in the Discussion section.

Summary of Lastarria-Lazufre Depth Profile

We have summarized all of the available observations for the Lastarria-Lazufre magmatic system in Table 3. Given currently available data sets, Vs is lower in the shallow crust beneath Lastarria than at Uturuncu; so we expect the heat flow to be higher (assuming thermal equilibrium and the composition is similar), and indeed the fumarole temperatures are higher (e.g., Table 1). If the low-resistivity and Vs region in the upper 6 km is dacite with >30% partial melt (Figs. 6A and 7D), the solidus curve in Figure 2 suggests a temperature of 660 °C—or hotter still, if the composition is andesite. This implies a heat flow of >700 mW/m^2. The temperature and heat flow could be lower if the seismic and MT anomalies are due at least in part to hydrothermal fluids and not partially molten rock.

DISCUSSION

The Plutonic-Volcanic Connection at Uturuncu and Lazufre

We now return to the question of the plutonic-volcanic connection that motivated the PLUTONS project. First of all, how do we identify a pluton or batholith in the subsurface? We do not have a simple or straightforward discriminator. For example, solidified batholiths can exhibit a high resistivity if they are composed of unaltered granite with low permeability (e.g., Comeau et al., 2015) or a low resistivity if hydrothermal circulation produced alteration and clay minerals. Low density in the subsurface can indicate solidified plutons, but the interpretation is non-unique (e.g., del Potro et al., 2013; Lipman and Bachmann, 2015). For a region that is currently partially molten, the geophysical anomaly could indicate country rock that has partially melted (i.e., a migmatite) or alternatively near-solidus igneous rock that will eventually become a batholith (e.g., Ward et al., 2014b). For the APMB, both interpretations are possible at different depths as part of a mature trans-crustal magmatic system. Based on the geophysical evidence for the presence of partial melt and the history of large ignimbrite eruptions in the region, many workers have concluded there is strong evidence for a large composite upper-crustal batholith beneath the APVC, but there are varying estimates of the volume and shape of this body or bodies (e.g., Zandt, et al., 2003; de Silva and Gosnold, 2007; Ward et al., 2014b; Kern et al., 2016). The PLUTONS data resolve some of these varying estimates.

When interpreting the geophysical observations in terms of the crustal-scale plutonic structure, we consider two end members developed at different trans-crustal magmatic systems around the world: (1) discrete depths of magma accumulation surrounded by country rock, including partially molten migmatite (Fig. 8C) or (2) a continuous composite batholith that extends through the entire crustal column (Figs. 8A and 8B). At Uturuncu, an interpretation based on a single geophysical measurement might (erroneously) appear to favor one end member over the other. At one extreme, the MT zones of low resistivity (e.g., C2 and C3, Fig. 9) are clearly separated by ~10 km, possibly suggesting separate zones of current or previous partial melt, such as in Figure 8C. At the other extreme, the regional sources of the ignimbrites (4–8 km below the surface, e.g., de Silva et al., 2006) could represent the top of the APMB. Thus, this entire region, from ~4 km to the bottom of the APMB ~30 km below the surface, is interpreted to be igneous rock that forms a batholith (Burns et al., 2015; Ward et al., 2014b; similar to Fig. 8A).

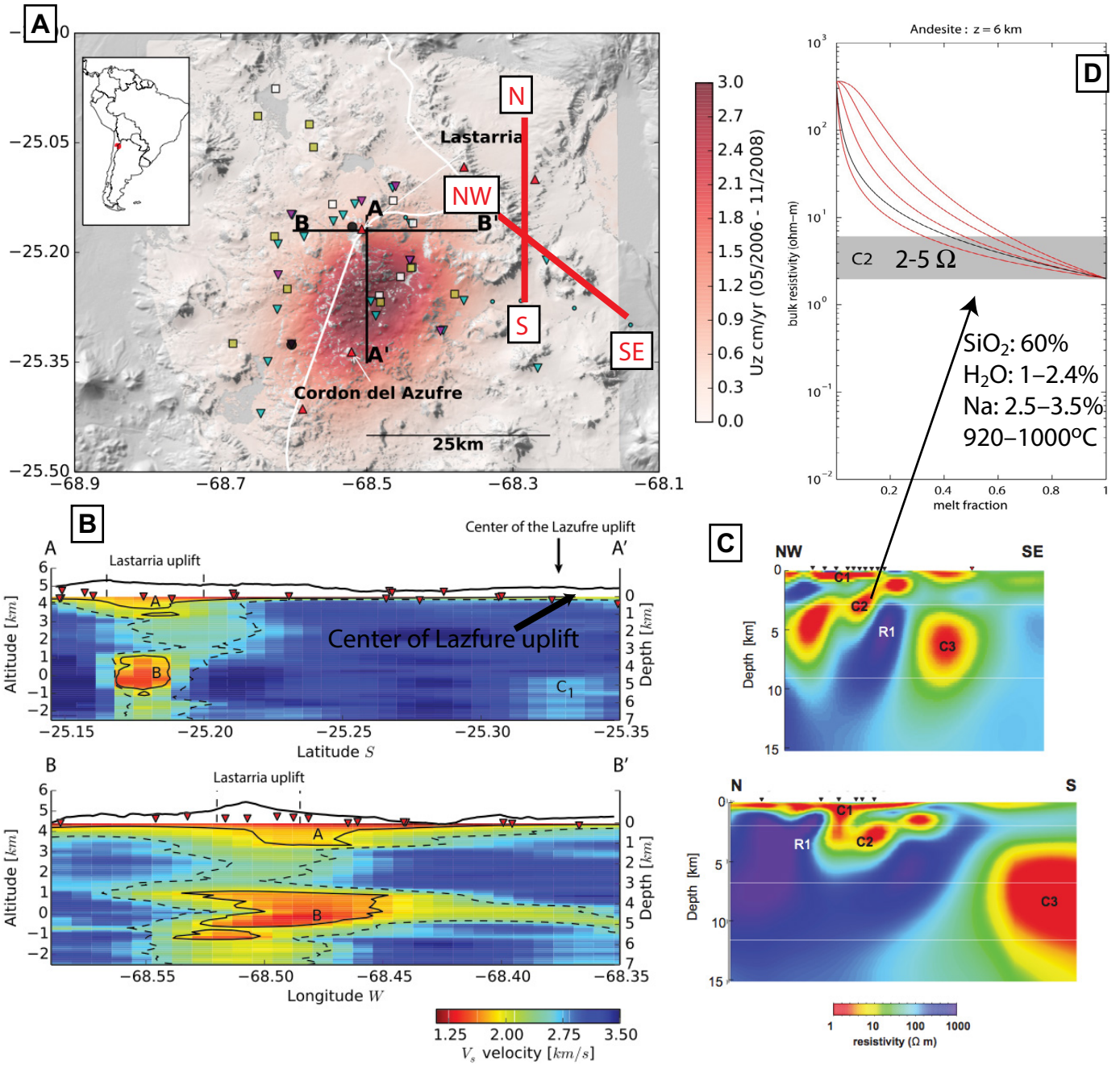

Figure 7. Geophysical observations and models at the Lazufre-Lastarria magmatic system. (A) Inferred vertical deformation from 2006 to 2008 (Remy et al., 2014). Squares show campaign GPS sites (white from Remy et al., 2014, and yellow from Henderson et al., 2017); inverted triangles show PLUTONS seismic stations (e.g., Spica et al., 2015); circles are PLUTONS magnetotelluric (MT) sites; and red triangles are Holocene volcanoes from the Smithsonian Institution. Reference map in the upper-left corner. Profiles from ambient noise seismic tomography (in black and shown in B) and MT inversions (in red and shown in C). (B) Vs from seismic tomography shown in black line profiles (A–A′ and B–B′) in (A) from Spica et al. (2015). (C) MT inversion profiles from the red line profiles (NW-SE and N-S) in (A) from Díaz et al. (2015). (D) Inferred partial melt based on resistive anomaly C2 in (C) using the method of Comeau et al. (2016) and parameters of possible andesitic composition (shown in subpanel) from Stechern et al. (2017). Inferred partial melt to match the observed resistivity from dacite is even higher (not shown).

TABLE 3. INTERPRETATION OF SUBSURFACE FEATURES IN THE LASTARRIA-LAZUFRE MAGMATIC SYSTEM USING OBSERVATIONS FROM FIGURE 7

Depth	Observations	Interpretation
Surface	Fumaroles at 80–408 °C (Aguilera et al., 2012; Zimmer et al., 2017); total volatile flux is 12,400–13,500 t/d (Tamburello et al., 2014; Lopez et al., 2018).	Liquid sulfur flows (Naranjo, 1985, 1988) imply episodes of higher temperatures.
~1 km below average surface: hydrothermal system	Minimum Vs ~1.8 km/s (Spica et al., 2015); MT <1 Ωm (Díaz et al., 2015); associated with depth of Lastarria deformation source (Froger et al., 2007).	Low Vs and resistivity features could be argillic clay altered cap on top of a higher-temperature hydrothermal system at greater depth.
3–6 km below average surface: magma chamber	Minimum Vs ~1.25 km/s (Spica et al., 2015); MT <10 Ωm (Díaz et al., 2015).	Seismic velocity implies 26%–31% partial melt (Fig. 6A; Spica et al., 2015) and MT >40% if only andesite (Fig. 7D). High concentrations of HCl and HF suggest a relatively shallow magma degassing depth (Tamburello et al., 2014; Lopez et al., 2018) consistent with this shallower reservoir.
7–15 km below average surface: deep magma reservoir beneath Lazufre	Source of Lazufre deformation in this depth range (e.g., Pearse and Lundgren, 2013; Remy et al., 2014). Geobarometry infers two main zones of storage from 6.5–8 km and 10–18 km depth plus sources >20 km deep (Stechern et al., 2017). Receiver functions show a low-velocity zone between 5–10 km bsl (McFarlin et al., 2014).	From MT: 5%–8% partial melt (Budach et al., 2013); This reservoir is beyond the limit of the network detection threshold of Spica et al. (2015) and Díaz et al. (2015), but appears on regional studies (e.g., Delph et al., 2017). The upper part of the low-velocity zone could contribute to open-system degassing, assuming a volatile saturated magma.

Abbreviations: bsl—below sea level; MT—magnetotelluric.

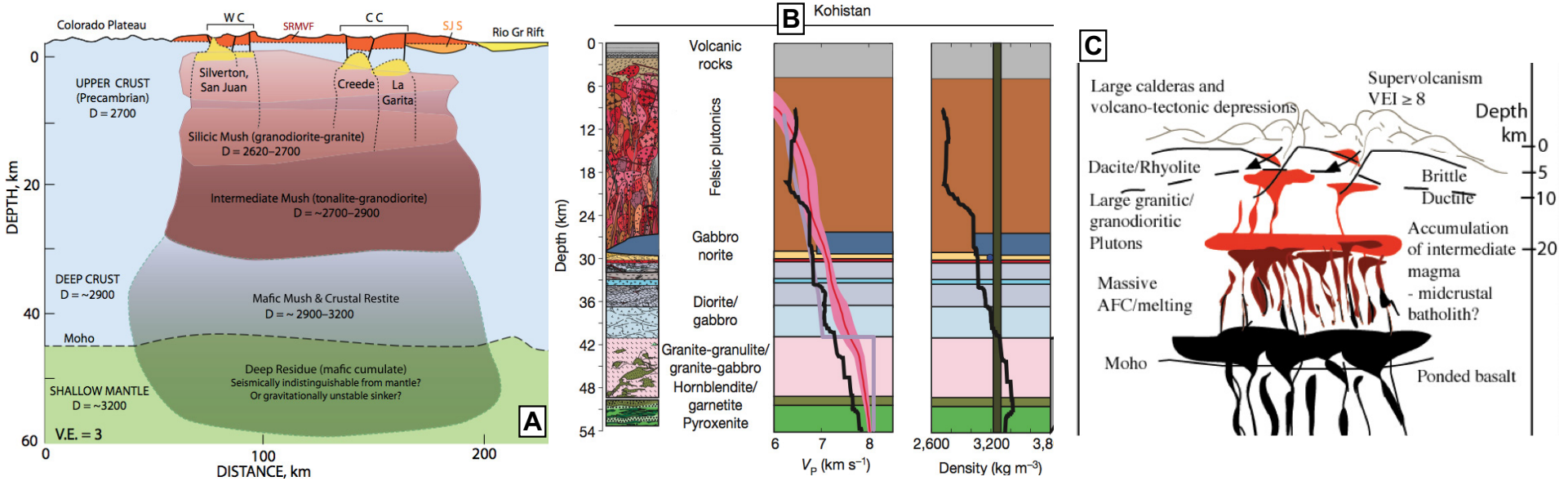

Figure 8. Interpretive cross sections showing end members of continuous zones of partial melt through the whole crustal column (A and B) and a model with partial melt at discrete levels with a more heterogeneous crust at in-between depths (C). (A) Inferred crustal section for the Southern Rocky Mountain Volcanic Field (SRMVF) that is east-west near 38°N from Lipman and Bachmann (2015) based on combined volcanologic, petrologic, and geophysical data. Yellow zones show top of shallow plutons presumed to be related to ignimbrite-forming eruptions, outlined by dotted lines, and corresponding to clusters of calderas (CC—central caldera cluster and WC—western calderas). (B) One-dimensional crustal section from the Kohistan arc, Pakistan, as mapped in the field (left) with interpreted composition, Vp (middle black line), and density (right, black line) from Jagoutz and Behn (2013) and references therein. In the middle, the pink and purple lines indicate seismic velocities measured in the Izu-Bonin arc and inferred from average continental crust, respectively. On the right, the vertical line shows the density of the upper mantle; so densities above that value are negatively buoyant. (C) Interpretive cross section of the Central Andes after de Silva et al. (2006). Abbreviations: AFC—Assimilation and Fractional Crystallization; SJS—San Juan sag; V.E.—vertical exaggeration; VEI—Volcanic Explosivity Index.

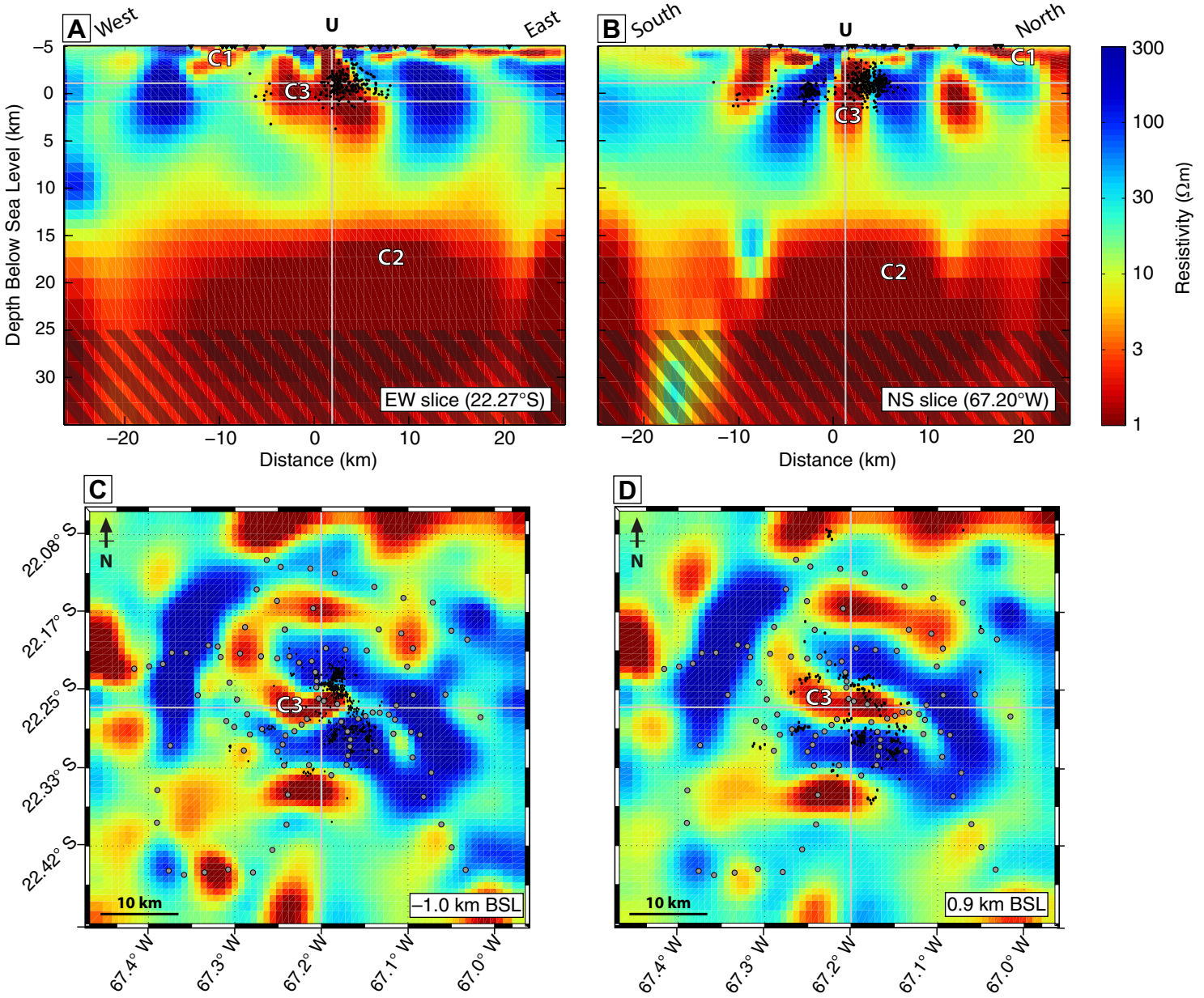

Figure 9. Shallow portion of 3D magnetotelluric (MT) inversion at Uturuncu from Comeau et al. (2016). (A) and (B) show west-east and south-north vertical slices and (C) and (D) show horizontal slices at two different depths, where the location of the 96 MT stations used in the inversion are shown as gray circles. Black dots show earthquake hypocenters from Jay et al. (2012). The hatched pattern shows the skin depth limit for electromagnetic signals (1000 s period); below this limit, features in the model are not well resolved.

Of course, these end members are both simplifications—for example, the vertically continuous batholith shown in Figure 8A was inferred from gravity data, and this type of data analysis has reduced resolution and may not image vertically elongate plutons separated by country rock (Lipman and Bachmann, 2015, and references therein). We favor an interpretation with elements of both end members at Uturuncu (Figs. 2 and 5), where a large batholith has been formed from an ensemble of plutons (e.g., Fig. 8B; Ward et al., 2014b, 2017), but with lateral heterogeneity in the upper 18 km (at least) resolved by the gravity and MT (Figs. 4B and 4C), but not by seismology (although there are hints of upper-crustal variability in Figs. 4E and 4F; Jay et al., 2012). We revise the Ward et al. (2014b) interpretation of a single continuous batholith from ~2–30 km below the surface to instead include (in the upper 18 km at least) igneous material surrounded by unmelted and partially melted country rock at scales that are seen in the field (Fig. 8B; Jagoutz and Schmidt, 2012; Fig. 4 of Paterson et al., 2011), inferred from geochemistry (e.g., Sparks et al., 2008; Michelfelder et al., 2013, 2014) and geochronology (e.g., Schmitt et al., 2003; Kern et al., 2016), but are not well resolved by the available geophysical data. Even after the ~10 m.y. of existence and extensive magmatic processing of the APVC, the APMB has not completely obliterated all traces of country rock. The consequence of our interpretation is the intruded:extruded ratio is likely below the 35:1 extreme from Ward et al. (2014b, their figure 7); although see Tierney et al. (2016) for a 75:1 petrological estimate in the region. Because we do not yet have a good discriminant between what is country rock versus igneous rock that is part of the batholith between 2 and 30 km depth, we cannot estimate this ratio.

Focusing on just the upper 10 km, we can relate erupted products to geophysical anomalies of potential plutonic origin. At Uturuncu, there are several EW zones of high and low resistivity that all extend from ~3 km above sea level to 3 km bsl and are ~15 km long and ~4.5 km wide (Fig. 9). If the anomalies signify solidified or partially solidified dacite, their total volume >1000 km^3, compared to the Uturuncu erupted volume of 80 km^3 (Sparks et al., 2008), provides an intrusion:extrusion ratio of >12:1, at the low end of the values proposed by Ward et al. (2014b). We interpret the pattern of high- and low-resistivity zones around Uturuncu as a propylitic hydrothermal alteration (e.g., Sillitoe, 2010) of varying permeability, temperature, and clay composition with tectonically controlled upflow of low pH magmatic fluids and regional inflow of neutral pH groundwater. A possible analogy of such an active zone of hydrothermal alteration imaged with MT is described by Gíslason et al. (2015), although the Uturuncu pattern is more complex. We do not think that the EW low-resistivity features are dikes as proposed by Comeau et al. (2016). The high-resistivity zones could be a shallow pluton related to intrusion of dacite magma, whereas the low-resistivity zones are attributed to saline fluids and hydrothermal alteration. Note that zones more distant from the summit of Uturuncu appear smoother because in those regions there are fewer MT stations.

For the Lastarria-Lazufre magmatic system, the end member of Figure 8C depicting discrete magma bodies is likely more appropriate than the continuous pluton (Figs. 8A and 8B). Geophysical inversions indicate isolated pockets of partially molten rocks at different depths that are separated presumably by country rock or solidified plutonic rock (Figs. 7B and 7C). The volume of the seismic anomaly from 3 to 6 km is 81 km^3, compared to the Lastarria erupted volume of ~10 km^3, also suggesting an intruded:extruded ratio (8:1) at the low end of the range of Ward et al. (2014b). For Lazufre, Naranjo et al. (2018b) estimated a lava volume of 35 km^3 that has erupted since 0.4 Ma with another 85 km^3 of lava erupted between 3.5 and 0.5 Ma, compared to the partially molten volume estimate of Remy et al. (2014) >400 km^3 (or 2769 km^3 for the best-fitting model)—providing a range of intruded:extruded ratio from 3:1 to 23:1.

The difference between Lazufre (more similar to Fig. 8C) and Uturuncu (more similar to Figs. 8A and 8B) could reflect these two different systems being at different stages in their evolution as mentioned above—Uturuncu and the APMB are mature, and activity is waning; while the SPMB and Lazufre are less mature, and activity could be increasing in the area, such that the zones of partial melt beneath Cerro Galán, Lazufre, and the southern terminus of the active arc (Fig. 1B) might eventually coalesce into an APMB-like magma body. Alternatively, perhaps the amount of melting will never be as extreme in the SPMB as the APMB because it is tectonically and compositionally distinct such that the crust is less fertile for melting, or the heat source is smaller (e.g., Beck et al., 2015). Certainly there is no evidence at Lazufre for a major magmatic flare-up such as the APVC ignimbrite province within which Uturuncu developed, although there is a long history of explosive volcanism and tectonomagmatic interaction (Naranjo et al., 2018a).

Future Eruptions at Uturuncu and Lazufre?

Considering that neither Uturuncu nor Lazufre are unambiguously associated with a Holocene volcano, the eruptive threat from these deformation centers is unclear. Uturuncu was the first area of active ground deformation observed at a Pleistocene or older volcano, but now a handful of these are known, including Sillajhuay in the Central Andes (Pritchard et al., 2014a) and elsewhere (e.g., Africa: Biggs et al., 2013; or New Zealand: Hamling et al., 2016). These features have been called "zombie volcanoes" by a headline writer of a popular science news Web site because they are "alive" even though they appear "dead" (Pritchard et al., 2014b).

We argue that Sillajhuay and Uturuncu should be added to the list of potentially active volcanoes, both because of their current activity and the fact that volcanoes in the Central Andes can have >10^5 years between eruptions (e.g., Clavero et al., 2004; Klemetti and Grunder, 2008). Sparks et al. (2008) noted that given the long time interval since the last eruption at Uturuncu and the evidence for ongoing magma intrusion from the ground deformation, there was the potential for a large eruption, perhaps even a caldera-forming eruption. But there is still no geophysical evidence for the shallow accumulation of eruptible magma at Uturuncu or Sillajhuay that could lead to eruption in the near future. In contrast, there are currently potentially small volumes of magma near the surface in the Lazufre-Lastarria system (e.g., Tamburello

et al., 2014; Spica et al., 2015; Lopez et al., 2018). However, these shallow accumulations may not be relevant because there is increasing evidence that prior to some caldera-forming eruptions, large volumes of silicic magma are transferred into shallow crustal chambers from much deeper in only decades to centuries (e.g., Druitt et al., 2012; Allan et al., 2013). In any case, we recommend continued vigilance at these potentially active volcanoes, to better understand their background levels of activity and characterize temporal changes.

Conceptual Models for Deformation at Uturuncu and Lazufre

How does the ground deformation at Uturuncu and Lazufre relate to the model of batholith formation and eruption potential discussed above? Previous work inferred that a magma intrusion was the most likely cause of deformation because of the deep sources at Lazufre (8–14 km below the surface; e.g., Pearse and Lundgren, 2013; Remy et al., 2014) and Uturuncu (6–19.5 km below the surface; e.g., Hickey et al., 2013, and Gottsmann et al., 2017). The hydrothermal systems are considered to be shallower (e.g., Pritchard and Simons, 2002; Sparks et al., 2008). If the volume changes are assumed to be due to magma intrusion, then the present-day rate (~10^{-2} km^3/yr or 1 m^3/s at Uturuncu) is much higher than the long-term eruptive average (~6×10^{-5} km^3/yr at Uturuncu; Muir et al., 2015). Similarly, the rate of inferred magmatic intrusion at Lazufre (~7×10^{-3} km^3/yr; Henderson et al., 2017) is more than two orders of magnitude higher than the long-term average since 4 Ma (~3×10^{-5} km^3/yr; Naranjo et al., 2018b). The putative magma intrusion must therefore be short-lived and is consistent with a model of batholith growth by numerous increments of magma addition over millions of years (e.g., Coleman et al., 2004; Glazner et al., 2004).

However, as described above, the lack of geomorphic uplift over the past 16,000 years at Uturuncu and Lazufre causes us to consider alternatives to the model of magma intrusion as the cause of the surface deformation. To produce effectively zero net deformation over millennia, uplift from magma injection and/or melting of surrounding country rock (i.e., anatexis that involves a significant volume change; e.g., Fialko et al., 2001) would have to be balanced by equal subsidence from cooling and crystallization of the new magmatic intrusion and surrounding country rock including processes such as "reverse diapirism," where mafic cumulates in a magma reservoir cause sinking (e.g., Roman and Jaupart, 2016). These subsidence mechanisms may be occurring at calderas that have been subsiding for decades without eruption, such as Cerro Blanco in the Central Andes (Henderson and Pritchard, 2013) and elsewhere (e.g., Parker et al., 2014). However, to get the uplift and subsidence to be nearly equal requires a narrow range of parameter space as demonstrated by viscoelastic and thermoelastic modeling including crystallization in the case of the Socorro magma body, New Mexico (Pearse and Fialko, 2010). This narrow range of parameters, while possible, may not be very likely.

An alternative conceptual model is that supercritical fluids from the partially molten zones at depths >10 km at Lazufre and Uturuncu could become temporarily trapped, causing pressurization of a subsurface reservoir and ground uplift (e.g., Gottsmann et al., 2017). Such a model has been proposed for Soufriére Hills Volcano, Montserrat (Christopher et al., 2015; Sparks and Cashman, 2017), although these papers do not explore the implications of the model for ground deformation. At Uturuncu, this pressurization would occur in a column above a bulging andesitic APMB (with a base at ~18 km below the surface; Fig. 4; Table 2) and would occur at the same time that lateral depressurization occurred in the APMB—the result would be the distinct pattern of uplift surrounded by a moat of subsidence observed (Gottsmann et al., 2017). At Lazufre, the gases might be only partially trapped, since there is a significant flux of gas out of Lastarria (Tamburello et al., 2014; Lopez et al., 2018).

The impact of the gas pressurization and/or depressurization cycles on ground deformation are likely to be of equal magnitude due to mass conservation, creating no net geomorphic deformation. In fact, such an equal and opposite pattern of uplift and subsidence was seen in the Central Andes at Cerro Overo between 1992 and 2011 (Henderson and Pritchard, 2013) where deformation changed sign over a short timespan (years or less), which would be more consistent with gas movement than bulk thermodynamic, thermoelastic, and viscoelastic processes. Compared to Uturuncu, the Cerro Overo deformation has a smaller maximum amplitude (~4 cm) and rate (~0.5 cm/yr), temporal and spatial scale (<10 years for a pulse of uplift or subsidence spanning 20 km diameter), perhaps explained by its location on the periphery of the APMB (with lower melt and gas content), while Uturuncu is near the center (Fig. 1A).

Whether the current uplift pattern at Lazufre will be counterbalanced by subsidence in the future is not clear—while there is geomorphic evidence for a 500 m topographic swell associated with the Lazufre uplift and radially oriented volcanic vents formed ca. 0.4 Ma, net uplift over the past ~16,000 years is negligible (figure 2 in Perkins et al., 2016a). Is the current Lazufre uplift an intrusion that will cause net uplift consistent with the long-lived topographic swell, or is it a transient feature that will produce no net deformation over timescales of centuries to millennia? We favor the latter interpretation for two reasons: (1) the topographic swell does not seem to have been growing during the recent millennia, and (2) although the current uplift and the swell are in the same location, the current uplift has a radius that is 10–15 km smaller than the swell (Perkins et al., 2016a), suggesting that different processes or source depths could be responsible. The difference between current uplift and the regional topographic anomaly is also true at Uturuncu—the ~70 km regional uplift is much smaller than the ~230-km-diameter, 1-km-amplitude regional topographic anomaly associated with the APMB (Perkins et al., 2016b). While it is possible that repeated uplift events such as those at Uturuncu and Lazufre could build the observed larger topographic features if the centroid of deformation moved around, the lack of any deflected geomorphic features in the past 16,000 years (Perkins et al., 2016a) leads us to suggest that the process or processes contributing to the creation of the 0.5–1 km topographic features have not been active over the past millennia at these two sites.

Although the millennial-scale deformation has only been studied at a few volcanic systems, there seem to be alternating episodes of uplift and subsidence that produce little net deformation in areas of current active deformation, such as Yellowstone and Socorro (e.g., Pierce et al., 2002; Finnegan and Pritchard, 2009). On the other hand, we know that such episodes of net deformation do occur with timescales of centuries to millennia at restless calderas (e.g., Campi Flegrei, Cinque et al., 1985; Laguna del Maule, Chile, Singer et al., 2015) and resurgent calderas (Kaizuka et al., 1989; Chen et al., 1995; Kennedy et al., 2012; de Silva et al., 2015). Based on recent crustal volcanism in the Central Andes, we suspect that episodes of magma intrusion in the middle crust (that could be related to batholith formation as described above) and surface uplift are still occurring in the region, but that these intrusions have not yet been observed in real time. We therefore propose that intrusions that cause long-term uplift are less common than uplift from pressurization by magmatic fluids and that gas and/or volatile processes are the cause of the five uplifting and/or subsiding areas in the Central Andes between 1992 and 2016 (e.g., Pritchard and Simons, 2004; Henderson and Pritchard, 2013; Pritchard et al., 2014a). Of course, some process is needed to cause the proposed change in volatile movements, and one such mechanism is mush destabilization as proposed by Sparks and Cashman (2017) driven by intrusion or inherent instabilities in the system. Further numerical modeling is needed to determine if these processes would still cause net geomorphic uplift or be nearly volume neutral.

Following our proposed conceptual model, the observed ground deformation at Uturuncu and Lazufre and most other deformation sites in the Central Andes (e.g., Putana, Cerro Overo, and Sillajhuay) is not fundamentally part of the process of batholith creation but is a consequence of large bodies of partially molten rock in the mid-crust releasing volatiles. These volatile phases are important for the generation of ore bodies (e.g., Hedenquist and Lowenstern, 1994; Cloos, 2001; Einaudi et al., 2003; Ingebritsen et al., 2010; Blundy et al., 2015; Weis, 2015). If correct, this conceptual model suggests that deformation could occur over any large zones of partial melt that are exsolving volatiles where the volatiles do not have a direct path to the surface and can undergo periodic trapping and release. This hypothesis would predict that if we looked over a longer time period, other areas above zones of partial melt in the Central Andes would show uplift and subsidence. We suggest that any of the topographic swells of similar scale to Lazufre seen in the long-wavelength topography of Figure 1 of Perkins et al. (2016a), including Putana, Llullaillaco, Cerro Galán, Cordón de Puntas Negras, El Queva, Antofalla, etc., could host partial melt and ground deformation.

In fact, there are several signs of activity in these areas—bursts of uplift and seismic activity have been seen at Putana (Pritchard et al., 2014a), uplift and subsidence at Cordón de Puntas Negras (at Cerro Overo; Henderson and Pritchard, 2013), as well as seismic swarms at Cerro Galán (Mulcahy et al., 2014). One potential trigger for these bursts could be shaking from subduction zone earthquakes (as proposed for the 1998 onset at Lazufre by Pritchard and Simons, 2002), but not all earthquakes impact changes in ground deformation (e.g., Henderson and Pritchard, 2017); therefore, the link is still speculative.

Regional and Global Context for Uturuncu and Lazufre

Ground Deformation

The seven large deformation patterns in the Central Andes (Uturuncu, Lazufre, Hualca Hualca, Cerro Overo, Cerro Blanco, Putana, and Sillajhuay) have rather simple ellipsoidal shapes whose centers do not move significantly over years to decades, unlike the patterns in some other areas of silicic magmatism, where the pattern, loci, and sign of deformation are more variable (e.g., Yellowstone: Wicks et al., 2006; and Cordón Caulle: Jay et al., 2014). We interpret the simpler deformation patterns in the Central Andes to reflect less spatial heterogeneity in the magma storage systems at least over the time period of observation—the ground deformation at Cordón Caulle and Yellowstone is caused by shallower magmatic sources (~5–10 km below the surface) that provide thermal energy to shallow hydrothermal systems that could be more extensive in those areas with more ground water than the arid Central Andes. For comparison, Yellowstone Caldera is thought to have a magma reservoir with a volume of ~46,000 km^3 partial melt (Huang et al., 2015), while Ward et al. (2014b) estimated that the APMB contains a partially molten region of ~500,000 km^3. Among the locations undergoing deformation in the Central Andes and globally, the Uturuncu deformation is unique in having a moat of subsidence, which is attributed to the large partially molten zone beneath the volcano (Gottsmann et al., 2017). Although the Putana uplift is also near the APMB, it is much shallower, probably related to the hydrothermal system—which raises the question of whether the Uturuncu hydrothermal system also undergoes deformation. Deformation caused by the Uturuncu hydrothermal system has not yet been observed (although see Lau et al., 2017).

Surface Temperature and Fumaroles

Movements of magmatic fluids and gases have been proposed as the cause of ground deformation at Uturuncu and Lastarria-Lazufre, and both areas have fumarolic fields. Uturuncu has one of the largest satellite-detected hotspots and fumarolic fields in the Central Andes in terms of surface area (Fig. 10; Jay et al., 2013) and is the only hotspot at a Pleistocene volcano in the region. At Lazufre, there are no active fumaroles yet detected near the center of the Lazufre deformation (e.g., Pritchard and Simons, 2004; Jay et al., 2013), but the nearby Lastarria volcano has a well-studied fumarolic field (e.g., Naranjo and Cornejo, 1992, 2010; Aguilera et al., 2012; 2016; Lopez et al., 2018) and satellite-detected thermal anomaly (Jay et al., 2013). It has been suggested that the Lastarria fumarole field serves as a pressure valve for Lazufre (Froger et al., 2007).

The Uturuncu and Lastarria satellite detected hotspots, and in fact all volcanic hotspots in the Central Andes and their associated thermal features (fumaroles, hot springs, geysers, etc.), are restricted to areas with a spatial extent of a few km^2 (Jay et al., 2013). In comparison, satellite hotspots and ther-

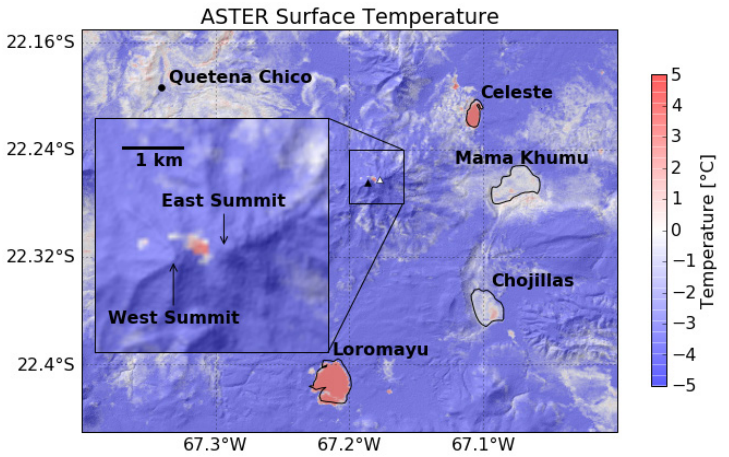

Figure 10. Night-time temperatures at Uturuncu measured on 9 November 2009 by the advanced spaceborne thermal emission and reflection radiometer (ASTER) instrument on the Terra satellite, processed at the Land Processes Distributed Active Archive Center (LPDAAC) to product 8 (surface kinetic temperature) draped over 30 m Shuttle Radar Topography Mission (SRTM) shaded relief with lakes outlined and labeled. Each pixel is 90 m², and the hotspot shows up as a region of ~50 pixels (~4500 m²) within the saddle between the two Uturuncu summits, with temperatures elevated ~15 K above the cold, blue background temperatures at higher elevation. Fumarole temperatures on the ground have been recorded (see references in Jay et al., 2013). Night-time ASTER images have imprecise georectification, and this image was shifted to align the image with the lake outlines by –0.0075° of longitude and –0.0025° in latitude.

mal features at Cordón Caulle and Yellowstone have areas greater than 10 km² (e.g., Vaughan et al., 2012; Jay et al., 2013). As with the deformation patterns, the thermal characteristics of Cordón Caulle and Yellowstone suggest those systems are more active at shallower depths than Uturuncu and Lazufre, with significant lateral heterogeneity.

Samples from the Lastarria hydrothermal system show evidence for mixing of (1) saline fluids superheated, by a deep, magmatic source that was ultimately derived from mantle melting ($^3He/^4He$ ratio of 4–6 times the average atmospheric composition) with (2) cooler, shallower, less saline groundwater (Aguilera et al., 2012, 2016; Lopez et al., 2018). The emission rate of SO_2 was measured by mini–differential optical absorption spectroscopy (DOAS) by Tamburello et al. (2014) in 2012, and in 2014 using several techniques by Lopez et al. (2018), who measured gas composition with the MultiGAS instrument to calculate the total emission rate of all volatiles of ~12,400–13,500 t/d. The high flux of SO_2 and the CO_2/SO_2 ratio <2 are both consistent with shallow magmatic degassing. Temporal variations in several gas ratios (increase in H_2O/CO_2 and maybe HCl/S_t along with a decrease in CO_2/S_t and H_2O/S_t) between the first campaign measurements in 2006 and the most recent in 2014 suggest a drying out of the hydrothermal system and an increase in degassing of magma soluble gases with time. Lopez et al. (2018) interpret this as evidence for magma ascent between 2006 and 2012–2014 or isobaric crystallization-induced degassing of a stalled magma body.

In contrast, there are no published reports on the gas discharge from Uturuncu. One argument against the role of gas in causing deformation is that the gas release at Uturuncu is apparently low based on the surface appearance and limited measurements (see Appendix); but, perhaps the gas discharge is diffuse (as suggested by the large satellite thermal anomaly, Fig. 10), or the gas emission is episodic (as suggested for Montserrat, with several thousand years of discharge occurring in a few years; Christopher et al., 2015).

Shallow Earthquakes

While ground deformation and thermal anomalies can be measured from space at Uturuncu and Lazufre and compared, it is more difficult to compare the seismic activity of these volcanoes. Uturuncu and Lazufre are both hundreds of kilometers from the nearest permanent seismic networks, and there are no teleseismic events (M_w greater than ~5) with reliable depths recorded near these volcanoes (e.g., Devlin et al., 2012; Pritchard et al., 2014a). Local networks near both Lastarria and Uturuncu from the PLUTONS and related projects recorded hundreds of small events (M_w <3) and reveal a wealth of information about the processes occurring including volcanic tremor and low-frequency earthquakes (Lastarria only), earthquake swarms, non-double-couple earthquakes, and triggered seismicity (e.g., Jay et al., 2012; Alvizuri and Tape, 2016). Although there are fewer data available on shallow earthquakes at other volcanoes in the Central Andes, based on available reconnaissance-level observations, it seems that the seismic activity at Uturuncu and Lastarria is among the highest in the region (Pritchard et al., 2014a). In fact, to our knowledge, Uturuncu is the only seismically active, Pleistocene volcano in the Central Andes, although seismic activity has been detected near the Pampa Lirima geothermal project in the Central Andes (Arcos et al., 2011) and could be related to the Pliocene Sillajhuay volcano (Pritchard et al., 2014a).

Remaining Questions

There are some questions that the PLUTONS project was not able to answer and new questions that have been raised by the research. Below, we describe these questions and suggest new observations and models that are needed to provide answers.

Temporal Variations in Ground Deformation and Seismicity

A single GPS station at Uturuncu spanning 2010–2015 shows a variable rate of uplift (Henderson and Pritchard, 2017). Similarly, ground deformation at the Lastarria-Lazufre magmatic system is seen to vary in time over the past two decades (e.g., Henderson et al., 2017). Future InSAR observations that span a large enough region to sample the entire deformation field (e.g., from the Sentinel-1a and 1-b satellites) and more GPS data (including reoccupation of

campaign GPS sites installed by the PLUTONS project) are needed to better understand the temporal and possibly spatial variations in deformation that are used to inform models of the processes causing deformation. For example, our model of gas pressurization and/or depressurization suggests that subsidence of approximately equal magnitude to the uplift is needed to explain the lack of net geomorphic uplift at both Uturuncu and Lazufre and could occur in the coming decades.

There are no permanent seismometers near Uturuncu or seismic networks at Lazufre (although the Southern Andean Volcano Observatory [OVDAS] has two seismometers at Lastarria, on the Chilean side of the border), and so the characteristics and temporal variations in the earthquake activity at these volcanoes are not known. Jay et al. (2012) suggest some temporal variations at Uturuncu, but the data are very limited. In particular, it would be useful to understand if there are changes in the number, size, and type of earthquakes associated with the observed changes in ground deformation described in the last paragraph, or to determine if magma might be moving closer to the surface. We recommend installation of small, permanent, seismic networks near both Uturuncu and Lazufre.

Seismic and MT Anisotropy

Partially molten zones contain significant spatial heterogeneity that can be detected as anisotropy by seismic and electromagnetic (EM) wave propagation. To unravel the melt geometry and determine the amount of partial melt, observations of seismic anisotropy (e.g., Jaxybulatov et al., 2014; Spica et al., 2017), along with lab experiments and field observations, are required (e.g., Hammond and Kendall, 2016), and seismic anisotropy can also be used to understand the orientation of faults and fractures (e.g., Baird et al., 2015). Previous work in the APVC has suggested seismic anisotropy in the crust (Leidig and Zandt, 2003), particularly in the upper 7 km (Maher, 2017), as well as in the mantle (Sims et al., 2015), but further work is required, including studies at Lazufre. Magnetotelluric anisotropy has been studied in terms of understanding the need for a 3D inversion (e.g., Comeau et al., 2015, 2016; Díaz et al., 2015) but may also provide independent constraints on the amount of partial melt (e.g., as suggested for the mantle; Pommier et al., 2015). Even with the detailed observations from PLUTONS, the observations were logistically and financially constrained and so could be improved by better networks of geophysical observations (denser networks and/or spanning a larger spatial scale). For example, additional MT stations to establish a grid instead of profiles at both Uturuncu and Lazufre would help to better understand the 3D subsurface characteristics.

Expanded Data Collection at Lastarria-Lazufre

Since this area was the secondary target for the PLUTONS project, the study is only a reconnaissance effort. In particular, a denser network of stations spanning the international border is needed to better illuminate the earthquake activity and image the subsurface below the Lazufre uplift swell. A complete geochemical study of the Azufre, Cordón del Azufre, and Bayo complexes, including Los Colorados ca. 9 Ma ignimbrite and lavas within the caldera (Naranjo et al., 2018b), will help better determine the age of this complex structure, whether the volcanic vents are related, and the characteristics of the zone of melt generation (e.g., Froger et al., 2007; Perkins et al., 2016a).

Degassing Emissions and Composition

No constraints on gas composition or flux are available at Uturuncu (see Appendix), and only temporally discrete observations of these parameters are available at Lastarria. Considering our proposed model for ground deformation involves gas pressurization and/or depressurization, measuring the discharge of gases and their temporal variations would be important tests of this model. Specifically, measurements of diffuse degassing should be made at both Uturuncu and Lazufre and more broadly in the Central Andes, including deforming centers such as Cerro Overo (whose cycles of uplift and subsidence could also be related to degassing) and Cerro Blanco as well as non-deforming volcanoes.

Eruptive History of Volcanic Systems in the Central Andes

Uturuncu is one of the few volcanic centers in the region where the lava flows have been dated and their volumes have been measured to calculate the temporal variations in erupted volume. Do other centers above large zones of partial melt, such as the APMB and SPMB, show the same temporal variations, reflecting perturbations to these large zones of partial melt, or do they reflect smaller, individual characteristics (e.g., erosion or flank instabilities of the edifice promoting eruption)?

Joint Geophysical and Petrological Inversion

As demonstrated in Figure 2, by combining different geophysical inferences of the subsurface, we can understand the limitations of each individual data set to develop a unified model of subsurface characteristics. For example, a zone of low seismic velocity between 9 and 18 km below the surface of Uturuncu could have a relatively high resistivity if partial melt in that region is resistive dacite (e.g., Comeau et al., 2016). The next step forward is to combine various geophysical data sets including seismic, MT, and gravity data in a formal joint inversion that accounts for the different sensitivities of each technique (e.g., Moorkamp et al., 2011). But, for these joint inversions to succeed, we need experimentally determined relations between subsurface properties, such as composition, geometry, and the amount of partial melt and observations of seismic velocity, density, and resistivity. Laboratory measurements of rock properties have been extremely valuable—for example, they have shown that basaltic melts have lower resistivity than sometimes assumed (e.g., Pommier and Garnero, 2014) and that dacitic melt actually has a relatively high resistivity (Laumonier et al., 2015). However, laboratory experiments have not explored all relevant portions of parameter space and should consider the ef-

fects of three-phase systems on resistivity, Vp, Vs, including the role of CO_2 and other non-aqueous volatiles. Further, accurate assessment of the amount of melt must consider anisotropy (mentioned above) as well as the effects of smoothing on geophysical inversions that can underestimate melt percentages by more than 20% (e.g., Paulatto et al., 2012).

Geomorphology and Numerical Modeling

Our interpretation that the uplift at Uturuncu and Lazufre is related to cycles of gas pressurization and/or depressurization could be challenged by new observations or models. Specifically, new observations of net geomorphic uplift over the past several thousand years as found at Laguna del Maule, Chile (Singer et al., 2015) would challenge the gas pressurization and/or depressurization model. Because we currently do not have evidence of net uplift over these timescales, we think that a diapir model is no longer favored for Uturuncu (e.g., Perkins et al., 2016a), but future numerical models of diapir ascent may show decadal variations in uplift rate (e.g., related to spatial variations in melt fraction) that could produce no net deformation over millennia. In particular, we need self-consistent models that include not just movement of partial melt and pressurization and/or depressurization of reservoirs but those that model the deformation effects of thermal and thermodynamic consequences of fluid movements in a viscoelastic material—for example, anatexis, heating and then cooling of surrounding country rock and crystallization. These models would include the temperature and heat-flow evolution with time as activity in the shallow dacite chamber waxes and wanes; such activity can be compared with petrological and heat-flow measurements.

Temperature and Rheology

To constrain the numerical models described in the last paragraph, we need better constraints on the subsurface temperatures and rheology at both Uturuncu and Lazufre. Observations of heat flow in both locations are valuable and could be used to constrain different inferences about the subsurface including whether the physical cause of the low seismic velocity zones are caused by partial melt or something else (e.g., comparing 150 and 200 mW/m^2 lines in Fig. 2D). An independent constraint on the subsurface temperature could be provided by using Vp and Vs to determine the depth of the alpha-beta quartz transition or the Curie temperature, as done elsewhere (e.g., Hacker et al., 2014; Saibi et al., 2015). In terms of subsurface rheology, the viscosity of the partially molten zone can be estimated from the resistivity derived from the MT data (Comeau et al., 2016). However, the bulk effective viscosity on timescales of years to millennia is also needed for modeling the geodetic and geomorphic observations. This viscosity could be estimated by measuring the lithospheric response to unloading of large paleolakes, such as Lake Minchin, which is just to the north of the APMB (e.g., Bills et al., 1994). Finally, seismic attenuation (e.g., Farrell et al., 2017) could be used to estimate viscosity (e.g., Priestley and McKenzie, 2013).

Relationship between Uturuncu and the APVC Ignimbrites

The relationship between magmatism at Uturuncu and the ignimbrite-dominated activity of the APVC is not fully understood. The spatial and temporal connection between Uturuncu and the APVC is obvious, and the calc-alkaline high-K dacites and minor andesitic compositions erupted at Uturuncu share many characteristics with those of the APVC—that they are ultimately derived from APMB is not in question (Muir et al., 2014a, 2014b; de Silva et al., 2006). However, Michelfelder et al. (2014) showed that Uturuncu is an outlier compared to other Pleistocene arc front and other composite volcanoes in the CVZ. Bulk-rock isotope data and the Sr isotopes from plagioclase phenocryst cores from Uturuncu are more radiogenic compared to regional arc dacites and andesites but concordant with those from the APVC (particularly the eastern APVC ignimbrites, such as Panizos), although Uturuncu dacites do not share the peraluminous character of these ignimbrites. Model entrapment pressures based on plagioclase-hosted melt inclusions for Uturuncu (Muir et al., 2014a, 2014b) and those from quartz-hosted melt inclusions from APVC dacites (Schmitt et al., 2001; Grocke et al., 2018) show broad concordance with the ignimbrite magmas extending to slightly greater pressures. There are some important differences. Uturuncu's anhydrous assemblage of plagioclase, orthopyroxene, and biotite is a subset of the APVC magmas that typically have plagioclase, quartz, amphibole, and biotite with some units containing sanidine and others that contain orthopyroxene. These differences might be reconciled with local differences in the source and local storage regions, but these remain to be investigated, and the differences are not well understood. As also noted by Muir et al. (2014a, 2014b), the broad similarity of Uturuncu and APVC dacites brings to our attention that we need to better understand how "eruptions of vastly differing magnitude and energy can be sourced from magmas with similar compositions and similar dissolved volatile contents stored at similar depths in the upper crust."

Regional and Global Studies of Magmatic Systems

The PLUTONS project is one of a handful that has used a suite of detailed, coincident geochemical and geophysical observations to study the entire crustal expression of a magmatic system (e.g., see summary in Pritchard and Gregg, 2016). To better understand the significance of the results at Uturuncu and Lazufre, similar measurements are needed at other locations in the Andes and globally, to determine for example, how unique are the amounts and extent of partial melt? For example, are the low-velocity zones imaged in the lower crust extending from the APMB to perhaps the Moho (Kukarina et al., 2017) and the lower crustal reflector beneath Uturuncu (McFarlin et al., 2018) long-lived or transient features? Do they reflect a partially molten pathway that allows magma to ascend from the mantle to the mid-crust through porous flow as proposed for Hawaii (e.g., Pritchard et al., 2007), feeding the APMB? If so, has it always been located below Uturuncu, or does it move, depending on heat and melt supply from the mantle? Is the vertical anomaly from earth-

quake tomography below Uturuncu unique? Is this the only "feeder" to the APMB? Do other large partially molten zones (such as the SPMB) have a similar feature? Is this a long-lived feature, or does it move around over millions of years? Is there an APMB- or SPMB-like feature elsewhere in the northern Andes (Cotopxi or Nevado de Ruiz), southern Andes (Laguna del Maule or Cordón Caulle), or elsewhere in the world?

Note that if the APMB is mostly silicic and andesitic, then there must have been at least an equal volume of deeper lower-crustal complementary mafic and ultramafic cumulates—while some of this material may still be evident below the lower-crustal reflector observed by receiver functions (Fig. 5; McFarlin et al., 2018), some may have been lost by the delamination that is necessary to provide the heat to maintain a partially molten APMB for millions of years.

Some have posited that the APMB has been partially molten for the entire duration of the ignimbrite flare-up, although Babeyko et al. (2002) argue that to keep temperatures high enough in the mid-crust requires convection upwellings from the lower crust to transport heat from the mantle to the mid-crust. Maybe the low-velocity region imaged by Kukarina et al. (2017) shows the upwelling limb of the convection pattern in the lower crust that was suggested by Babeyko et al. (2002)? Partial melts moving upward would be partially compensated by the subsidence of dense refractory products of partial meting and fractional crystallization as envisaged in models of compaction and larger-scale crustal dynamics (e.g., Solano et al., 2012; Roman and Jaupart, 2016) that may be imaged by receiver functions in the lower crust (Fig. 5; McFarlin et al., 2018) at the bottom of the vertical low-velocity zone (Kukarina et al., 2017).

Alternatively, the uppermost APMB may have grown with time as reflected by the spatial, temporal, and volumetric pattern of ignimbrite eruptions through time (e.g., de Silva and Gosnold, 2007; Kern et al., 2016). Linking the record of the flare-up to the deeper APMB remains a challenge. An integrated numerical model of the evolution of the APMB over tens of millions of years constrained with PLUTONS data showing the newly imaged structures in the lower crust that could address the questions raised here has yet to be developed, and the fundamental ambiguity of the relevance of the geophysical observations to the >10 m.y. evolution of the APMB remains.

CONCLUSIONS

By combining multiple geophysical and geochemical methods, we have constrained the crustal-scale distribution of partial melt at Lazufre and Uturuncu. In the lower crust below Uturuncu, there is a 20–30-km-wide vertical low Vs zone (Kukarina et al., 2017) that possibly extends from ~40 km deep to the mid-crust, where it overlaps with the 200-km-diameter APMB. Beneath 40 km and the vertical low Vs zone is a zone of mafic cumulates in the mid- to lower crust that is visible on the receiver functions (McFarlin et al., 2018). We interpret the 7–10 km difference in depths between the top of the APMB from seismic tomography and/or receiver functions (Ward et al., 2014b) and from magnetotellurics to indicate that the APMB is compositionally zoned, with an upper region of dacitic melt (9–18 km below the surface) and andesitic melts below (18–30 km below the surface) (Fig. 2; Table 2). There are several zones of low resistivity between the APMB and the surface (Comeau et al., 2015, 2016), including one at ~5 km depth below Uturuncu itself; this zone is likely related to the current hydrothermal system developed in the region of the dacite magma chambers that supplied eruptions of Uturuncu before 250 ka (Muir et al., 2014a, 2014b, 2015). The presence of such a system and the likelihood that it contains brines may have implications for ore formation in this area because brines are known to strongly sequester and concentrate metals such as Cu and Mo (Candela and Holland, 1984; Simon et al., 2006; Frank et al., 2011; Zajacz et al., 2011; Tattitch et al., 2015; Tattitch and Blundy, 2017).

The PLUTONS project demonstrates the need for multiple geophysical and petrological techniques in order to constrain a crustal cross section such as that presented in Figure 2. All geophysical methods are non-unique (e.g., low seismic velocities can be caused by changing porosity, partial melt, composition, volatile content, temperature, attenuation, anisotropy, etc.), and some methods have "blind spots" (e.g., dacite melt has relatively high resistivity or MT cannot easily detect melt that is not well interconnected). Furthermore, the different geophysical techniques have different capabilities to resolve structures at different spatial resolutions—for example, long-wavelength seismic waves (Fig. 4D) averages over subsurface features that can be resolved by higher-resolution methods (Figs. 4C, 4E, and 4F), but these high-resolution methods may, in turn, miss the larger-scale structures (Fig. 4E). All geophysical techniques provide a snapshot of conditions in the subsurface at the present and raise questions about their temporal evolution (e.g., Ward et al., 2017). We do not know how the geometry of the APMB or SPMB has changed with time, except by inferences from the record of surface volcanic eruptions (e.g., Kay and Coira, 2009; Kern et al., 2016). Further, we do not know if structures imaged in the lower crust are long-lived or transient, but we have concluded that the "fossil dacite chamber" at Uturuncu once contained eruptible dacitic magma, although we do not think that there is partial melt there now—only an active hydrothermal system.

The Central Andes is unique among volcanic arcs in having very large zones of crustal partial melt (APMB and SPMB, total >0.5 million km^3) at >10 km depth. These zones are a product of the unusually thick crust and a history of subduction (e.g., Kay and Coira, 2010; Beck et al., 2015). Uturuncu and Lazufre are not the only deforming or seismically active volcanoes possibly related to these zones of partial melt, but they are globally unique in terms of the size of the deforming regions, the decadal timescales over which they have been deforming, and the ambiguous relationship between the deformation and seismic activity and Holocene eruptive centers. However, our observations of ground deformation in these areas span only a few decades, and considering the repose interval of $>10^5$ years, our interpretation of the cause of deformation requires a longer period of observation. This longer time period can be achieved through geomorphic observations of net uplift and subsidence or through the ergodic hypothesis that we can substitute space for time—which allows us to observe hundreds of other magmatic systems in dif-

ferent stages of their eruptive cycle to better understand the complete cycle. By combining these approaches, the PLUTONS project motivated a new interpretation for the cause of deformation. Because of the temporal variations in the deformation rate recorded by geodesy (e.g., Henderson and Pritchard, 2017; Henderson et al., 2017) and the lack of long-term uplift from geomorphology (Perkins et al., 2016a), we do not favor en masse diapiric movements. Instead, we suggest that the current uplift is a transient caused by exsolved volatiles that are being temporarily trapped at depths of up to 10–15 km and that will eventually be released with concomitant subsidence, causing no net deformation (Gottsmann et al., 2017). This model is consistent with other magmatic systems in the Central Andes such as Cerro Overo, which has been undergoing alternating periods of uplift and subsidence, or Cerro Blanco subsiding for decades (e.g., Henderson and Pritchard, 2013). This model can be tested by longer-term geodetic observations, time-series observations of total gas emissions, and viscoelastic numerical models of deformation that incorporate self-consistent compositional and thermodynamic characteristics and temporal evolution.

While Uturuncu and Lazufre share some characteristics with caldera systems such as Yellowstone and Cordón Caulle, there are significant differences in their manifestations of deformation, surface thermal features, and seismicity, possibly related to their hydrothermal systems, influence of faults, and the depth of partially molten rock. There might be partial melt at a depth of 3 km beneath Lastarria, but this needs to be tested with heat-flow observations. Furthermore, this magma chamber is relatively small (~81 km^3) and is on average <40% partial melt; so it is not considered eruptible (Spica et al., 2015). At Uturuncu, partial melt of ~10% may be present at 9 km depth (Ward et al., 2014b), but eruptible quantities do not exist in large volumes (e.g., Pritchard and Gregg, 2016). At this time, there is no indication that the large volumes of partial melt observed beneath Uturuncu or Lazufre will erupt in the future. However, further monitoring of these volcanoes, including the installation of permanent seismic arrays, is suggested to better understand the changing dynamics.

APPENDIX: DATA COLLECTED

Uturuncu

1. Gravity: 160 new survey (or static) benchmarks for a regional map (del Potro et al., 2013) and 25 sites that were reoccupied twice to assess temporal variations in gravity (called dynamic gravimetric data; Gottsmann et al., 2017).

2. Ground Deformation: Interferometric synthetic aperture radar time series from 1992 to 2011, two functioning continuous GPS, 2010–present (plus an additional site that was vandalized after one year; Henderson and Pritchard, 2017). GPS reoccupation in 2010 of leveling benchmarks from 1965 (Gottsmann et al., 2018).

3. Seismometry: 28 broadband seismometers from 2010 to 2012 (e.g., Farrell et al., 2017) have been used for: (1) joint receiver function and ambient noise tomography imaging using a subset of PLUTONS stations with others (Ward et al., 2014b); (2) earthquake tomography and earthquake locations (Kukarina et al., 2017); (3) P-wave attenuation and time delays (Farrell et al., 2017); (4) detailed studies of receiver functions using all PLUTONS data (McFarlin et al., 2018); (5) full moment tensors for 63 shallow events beneath the volcano (Alvizuri and Tape, 2016); and (6) a one-dimensional velocity model based on receiver functions, Rayleigh-wave horizontal-vertical amplitude ratios, and Rayleigh-wave phase velocities from earthquakes and ambient noise (Shen et al., 2017). A related project used 15 short- and intermediate-period seismometers at Uturuncu from 2009 to 2010, and Jay et al. (2012) describes earthquakes during that time and provides a 3D ambient noise tomographic map of Vs velocities in the upper 5 km.

4. Magnetotellurics: 180 broadband stations occupied for about one day per station during field campaigns in 2011, 2012, and 2013. Inversion for the subsurface resistivity structure was done using all stations in a 2D inversion (Comeau et al., 2015), as well as 73 (Comeau et al., 2015) and 96 stations (Comeau et al., 2016) in 3D inversions.

5. Geomorphology: Deflections of river longitudinal profiles and shorelines of lakes around Uturuncu were assessed with GPS and a 35 × 35 km 0.5 m/pixel photogrammetry-derived digital elevation model—selected shoreline features were dated using optically stimulated luminescence (Perkins et al., 2016a). Elevation of basement exposures and a long-wavelength uplift over the APMB have been analyzed to determine the extent of isostatic compensation and potential magmatic contributions to the modern surface topography (Perkins et al., 2016b).

6. Geochronology and Isotope Geochemistry: Kern et al. (2016) used in situ secondary ionization mass spectrometry (SIMS) analyses of U-Pb spot ages and trace elements in zircon to assess the magmatic evolution of 16 ignimbrites from the APVC for regional context. The volcanic output from Uturuncu has been constrained by 26 new $^{39}Ar/^{40}Ar$ plateau ages for 23 lavas and domes (Muir et al., 2015). Whole-rock analysis of 121 Uturuncu lava flow and dome samples for major- and trace-element concentrations were determined by X-ray fluorescence spectrometry (XRF). A subset of 60 samples was analyzed for trace-element concentrations including rare-earth elements by inductively coupled plasma mass spectrometry (ICP MS), Nd, Pb, and Sr isotopes by thermal ionization mass spectrometry (TIMS), and $\delta^{18}O$ values by laser fluorination (Michelfelder, 2015). Michelfelder (2015) provide major-, trace-element, and in situ Sr-isotope data on Uturuncu plagioclase phenocrysts combined with the whole-rock Sr-isotope ratios.

7. Petrology and Geobarometry: Grocke et al. (2018) analyzed samples from the 3.64 Ma Tara ignimbrite (from the 5.6–1.8 Ma Guacha caldera immediately south of Uturuncu) for whole-rock major and trace elements and isotopic compositions. Major- and trace-element concentrations of minerals, matrix glasses, and melt inclusions by electron microprobe, as well as the H_2O and CO_2 concentrations in quartz- and sanidine-hosted melt inclusions using secondary ionization mass spectrometry (SIMS), laser ablation (LA) ICP MS, and Raman spectroscopy have been analyzed. Muir et al. (2015) analyzed Uturuncu lavas for major-element concentrations of minerals, matrix glasses, and melt inclusions by electron microprobe, as well as the H_2O and CO_2 concentrations in plagioclase-hosted melt inclusions from lava flows by SIMS. Petrological phase equilibria experiments were run at a range of pressure and temperature conditions and compared with natural phase assemblages, modes, and mineral and glass compositions to understand the storage conditions of the dacitic magmas (Muir et al., 2014a, 2014b).

8. Gas Emissions: Measurements of gas flux and composition were attempted during the PLUTONS project but are not published elsewhere. We mention the available measurements here to motivate future work: Georg Zellmer (2011, personal commun.) took MultiGAS measurements in 2009 and noted diffuse degassing, with hundreds of tiny vents covering a large area close to the saddle of the mountain. He collected data during only a few brief periods that provide a rough estimate of the gas composition: CO_2 >6000 ppm (off scale); H_2S peaking at just above 80 ppm; SO_2 <170 ppm (though in most cases less than H_2S). Relative humidity went up to 100% (at 10 °C), confirming significant water in this otherwise dry region. In 2012, Taryn Lopez used a FLYSPEC (scanning ultraviolet spectrometer) at the highest seismic station on Uturuncu (1–2 km from the degassing area), but SO_2 was below the detection limit, implying the emission rate is probably less than ~10–15 t/d. The shallow hydrothermal system at Uturuncu could remove the highly water-soluble SO_2 from the gas phase and is consistent with the relatively high proportion of H_2S to SO_2. On the other hand, there is abundant sulfur on the surface at Uturuncu and a former sulfur mine a few km from the summit, suggesting higher deposition of sulfur in the past.

Lazufre-Lastarria

1. Seismology: Eight broadband seismometers deployed by PLUTONS from 2011 to 2013—a three-month subset of these data were combined with a two-month data set from 17 seismometers installed by Chilean and German researchers in 2008 (Spica et al., 2015) for ambient noise tomography mapping of the seismic shear-wave velocity variations beneath Lastarria. Analysis of these data for local earthquakes is ongoing (Heather McFarlin, 2018, personal commun.).

2. Magnetotellurics: The University of Alberta group collected 38 broadband MT stations in an EW profile through Lazufre during a field campaign in 2013. An additional 30 broadband MT sites from Díaz et al. (2015) and 11 broadband and long-period MT stations from Budach et al. (2013) focused around Lastarria are also included in the inversion (Comeau, 2015).

3. Geochronology and Field Mapping: During the past five years, the Chilean Geological Survey (Sernageomin) has created 1:100,000 maps along the volcanic arc between 25° and 27°S, including Lastarria and Lazufre, with 110 new $^{39}Ar/^{40}Ar$ ages to go along with the ~300 K-Ar ages from the 1990s (Naranjo and Cornejo, 1992; Naranjo et al., 2013).

4. Geomorphology: Perkins et al. (2016a) describe shorelines at a late Pleistocene lake near Lastarria volcano that could indicate the longevity of deformation. These authors also use the orientation of multiple dated lava flows to date the age of uplift of a topographic swell co-located with Lazufre, and they map the orientation of volcanic vents around the swell.

5. Ground Deformation: There are two functioning continuous GPS in the Lazufre deformation zone, with data between 2010 and 2014 at one station, and 2010–2015 at the other, plus a reference site 150 km from the deformation with data from 2011 to 2015 (Henderson et al., 2017). An additional reference site was vandalized, and useful data were not collected. There are ten campaign GPS sites installed by PLUTONS and occupied in 2012–2014, and seven other sites are also available from 2006, 2007, and 2008 from another project (Remy et al., 2014). An InSAR time series of ground deformation has been created from 1995 to 2011, and additional interferograms constrain deformation through 2016 (Henderson et al., 2017).

6. Petrology and Geochemistry: Lava flows were sampled at Lastarria (69 samples) and Cordón del Azufre (21), and the major- and trace-element geochemistry was studied by XRF, while a subset was analyzed for trace-element concentrations including rare-earth elements by ICP MS. Nd-, Pb-, and Sr-isotope ratios were measured by TIMS for 15 whole-rock samples (Wilder, 2015).

7. Gas Emissions: At Lastarria, fumarolic gases were sampled and analyzed by Aguilera et al. (2012) and Lopez et al. (2018), and vapor condensates and fumarolic solid samples (including fluid inclusions) were analyzed by Aguilera et al. (2016).

ACKNOWLEDGMENTS

Funding for this project was provided by the U.S. National Science Foundation through grants EAR-0908850 to N.J.F., EAR-0908324 to S.L. de S., EAR-0901148 to Todd Feeley, EAR-0909254 to University of Alaska, Fairbanks, and EAR-0908281 to Cornell with a subaward to the University of Alberta, the UK Natural Environmental Research Council (grant NE/G01843X/1), a Natural Sciences and Engineering Research Council of Canada (NSERC) Discovery grant awarded to M.J.U., and a Benjamin Meaker Visiting Professorship to M.E.P from the Institute for Advanced Study, University of Bristol. Total funding from all sources was about $4.5 million. We thank project collaborators who contributed to the project without direct PLUTONS funding. This project would not have been possible without the help of the Observatorio San Calixto, Bolivian Servicio de Areas Protegidas (especially the staff at the Reserva Eduardo Avaroa), the residents of Quetena Chico and Quetena Grande, the Servicio Nacional de Geología y Técnico de Minas, SERNAGEOMIN Chile, and our outstanding field drivers. We dedicate this paper and themed issue of *Geosphere* to the memory of our colleague and PLUTONS co-principal investigator, Todd Feeley (Michelfelder et al., 2016). We thank Robert Trumbull and an anonymous reviewer for critical reviews that improved the manuscript. Data from the PLUTONS project are archived for future use—seismic waveforms are at the IRIS Data Management Center, raw GNSS data are at UNAVCO, and access to other data sets are described in the respective papers.

REFERENCES CITED

Aguilera, F., Tassi, F., Darrah, T., Moune, S., and Vaselli, O., 2012, Geochemical model of a magmatic-hydrothermal system at the Lastarria volcano, northern Chile: Bulletin of Volcanology, v. 74, no. 1, p. 119–134, https://doi.org/10.1007/s00445-011-0489-5.

Aguilera, F., Layana, S., Rodríguez-Díaz, A., González, C., Cortés, J., and Inostroza, M., 2016, Hydrothermal alteration, fumarolic deposits and fluids from Lastarria Volcanic Complex: A multidisciplinary study: Andean Geology, v. 43, no. 2, p. 166–196, https://doi.org/10.5027/andgeoV43n2-a02.

Allan, A.S.R., Morgan, D.J., Wilson, C.J.N., and Millet, M.-A., 2013, From mush to eruption in centuries: Assembly of the super-sized Oruanui magma body: Contributions to Mineralogy and Petrology, v. 166, p. 143–164, https://doi.org/10.1007/s00410-013-0869-2.

Allmendinger, R.W., Jordan, T.E., Kay, S.M., and Isacks, B.L., 1997, The evolution of the Altiplano-Puna plateau of the Central Andes: Annual Review of Earth and Planetary Sciences, v. 25, no. 1, p. 139–174, https://doi.org/10.1146/annurev.earth.25.1.139.

Alvizuri, C., and Tape, C., 2016, Full moment tensors for small events (M_w < 3) at Uturuncu volcano, Bolivia: Geophysical Journal International, v. 206, no. 3, p. 1761–1783, https://doi.org/10.1093/gji/ggw247.

Annen, C., 2009, From plutons to magma chambers: thermal constraints on the accumulation of eruptible silicic magma in the upper crust: Earth and Planetary Science Letters, v. 284, p. 409–416, https://doi.org/10.1016/j.epsl.2009.05.006.

Arcos, R., Clavero, J., Giavelli, A., Simmons, S., Aguirre, I., Martini, S., Mayorga, C., Pineda, G., Parra, J., and Soffia, J., 2011, Surface exploration at Pampa Lirima geothermal project, Central Andes of northern Chile: Geothermal Resources Council Transactions, v. 35, p. 689–693.

Arndt, J., Bartel, T., Scheuber, E., and Schilling, F., 1997, Thermal and rheological properties of granodioritic rocks from the Central Andes, North Chile: Tectonophysics, v. 271, p. 75–88, https://doi.org/10.1016/S0040-1951(96)00218-1.

Babeyko, A.Y., Sobolev, S.V., Trumbull, R.B., Oncken, O. and Lavier, L.L., 2002, Numerical models of crustal scale convection and partial melting beneath the Altiplano–Puna plateau: Earth and Planetary Science Letters, v. 199, p. 373–388, https://doi.org/10.1016/S0012-821X(02)00597-6.

Bachmann, O., Miller, C.F., and de Silva, S.L., 2007, The volcanic–plutonic connection as a stage for understanding crustal magmatism: Journal of Volcanology and Geothermal Research, v. 167, p. 1–23, https://doi.org/10.1016/j.jvolgeores.2007.08.002.

Baird, A.F., Kendall, J.M., Sparks, R.S.J., and Baptie, B., 2015, Transtensional deformation of Montserrat revealed by shear wave splitting: Earth and Planetary Science Letters, v. 425, p. 179–186, https://doi.org/10.1016/j.epsl.2015.06.006.

Barazangi, M., and Isacks, B.L., 1976, Spatial distribution of earthquakes and subduction of the Nazca plate beneath South America: Geology, v. 4, no. 11, p. 686–692, https://doi.org/10.1130/0091-7613(1976)4<686:SDOEAS>2.0.CO;2.

Beck, S.L., Zandt, G., Ward, K.M., and Scire, A., 2015, Multiple styles and scales of lithospheric foundering beneath the Puna Plateau, Central Andes, *in* DeCelles, P.G., Ducea, M.N., Carrapa, B., and Kapp, P.A., eds., Geodynamics of a Cordilleran Orogenic System: The Central Andes of Argentina and Northern Chile: Geological Society of America Memoir 212, p. 43–60, https://doi.org/10.1130/2015.1212(03).

Bianchi, M., Heit, B., Jakovlev, A., Yuan, X., Kay, S.M., Sandvol, E., Alonso, R.N., Coira, B., Brown, L., Kind, R., and Comte, D., 2013, Teleseismic tomography of the southern Puna plateau in Argentina and adjacent regions: Tectonophysics, v. 586, p. 65–83, https://doi.org/10.1016/j.tecto.2012.11.016.

Biggs, J., and Pritchard, M.E., 2017, Global volcano monitoring—What does it mean when a volcano deforms?: Elements, v. 13, p. 17–22, https://doi.org/10.2113/gselements.13.1.17.

Biggs, J., Chivers, M., and Hutchinson, M.C., 2013, Surface deformation and stress interactions during the 2007–2010 sequence of earthquake, dyke intrusion and eruption in northern Tanzania: Geophysical Journal International, v. 195, no. 1, p. 16–26, https://doi.org/10.1093/gji/ggt226.

Bills, B.G., de Silva, S.L., Currey, D.R., Emenger, R.S., Lillquist, K.D., Donnellan, A., and Worden, B., 1994, Hydro-isostatic deflection and tectonic tilting in the Central Andes: Initial results of a GPS survey of Lake Minchin shorelines: Geophysical Research Letters, v. 21, p. 293–296, https://doi.org/10.1029/93GL03544.

Blundy, J., Mavrogenes, J., Tattitch, B., Sparks, R.S.J., and Gilmer, A., 2015, Generation of porphyry copper deposits by gas-brine reaction in volcanic arcs: Nature Geoscience, v. 8, p. 235–240, https://doi.org/10.1038/ngeo2351.

Brandmeier, M., and Wörner, G., 2014, Andes Ignimbrite Database, https://www.arcgis.com/home/item.html?id=47038ddc0628473f9f0ce67aa2eff8be.

Brandmeier, M., and Wörner, G., 2016, Compositional variations of ignimbrite magmas in the Central Andes over the past 26 Ma—A multivariate statistical perspective: Lithos, v. 262, p. 713–728, https://doi.org/10.1016/j.lithos.2016.07.011.

Brasse, H., Lezaeta, P., Rath, V., Schwalenberg, K., Soyer, W., and Haak, V., 2002, The Bolivian altiplano conductivity anomaly: Journal of Geophysical Research. Solid Earth, v. 107, p. 2156–2202, https://doi.org/10.1029/2001JB000391.

Brown, M., 2001, Crustal melting and granite magmatism: Key issues: Physics and Chemistry of the Earth, Part A: Solid Earth and Geodesy, v. 26, no. 4–5, p. 201–212, https://doi.org/10.1016/S1464-1895(01)00047-3.

Budach, I., Brasse, H., and Díaz, D., 2013, Crustal-scale electrical conductivity anomaly beneath inflating Lazufre volcanic complex, Central Andes: Journal of South American Earth Sciences, v. 42, p. 144–149, https://doi.org/10.1016/j.jsames.2012.11.002.

Burns, D.H., de Silva, S.L., Tepley, F., Schmitt, A.K., and Loewen, M.W., 2015, Recording the transition from flare-up to steady-state arc magmatism at the Purico-Chascon volcanic complex, northern Chile: Earth and Planetary Science Letters, v. 422, p. 75–86, https://doi.org/10.1016/j.epsl.2015.04.002.

Candela, P.A., and Holland, H.D., 1984, The partitioning of copper and molybdenum between silicate melts and aqueous fluids: Geochimica et Cosmochimica Acta, v. 48, no. 2, p. 373–380, https://doi.org/10.1016/0016-7037(84)90257-6.

Cao, W., Kaus, B.J.P., and Paterson, S., 2016, Intrusion of granitic magma into the continental crust facilitated by magma pulsing and dike-diapir interactions: Numerical simulations: Tectonics, v. 35, no. 6, p. 1575–1594, https://doi.org/10.1002/2015TC004076.

Chapman, D.S., 1986, Thermal gradients in the continental crust, *in* Dawson, J.B., Carswell, D.A., Hall, J., and Wedepohl, K.H., eds., The Nature of the Lower Continental Crust: Geological Society of London Special Publication 24, p. 63–70, https://doi.org/10.1144/GSL.SP.1986.024.01.07.

Chappell, B.W., White, A.J.R., and Wyborn, D., 1987, The Importance of Residual Source Material (Restite) in Granite Petrogenesis: Journal of Petrology, v. 28, no. 6, p. 1111–1138, https://doi.org/10.1093/petrology/28.6.1111.

Chen, J.K., Taylor, F.W., Edwards, R.L., Cheng, H., and Burr, G.S., 1995, Recent emerged reef terraces of the Yenkahe resurgent block, Tanna, Vanuatu: Implications for volcanic, landslide and tsunami hazards: The Journal of Geology, v. 103, p. 577–590, https://doi.org/10.1086/629777.

Chmielowski, J., Zandt, G., and Haberland, C., 1999, The central Andean Altiplano-Puna magma body: Geophysical Research Letters, v. 26, p. 783–786, https://doi.org/10.1029/1999GL900078.

Christopher, T.E., Blundy, J., Cashman, K., Cole, P., Edmonds, M., Smith, P.J., Sparks, R.S.J., and Stinton, A., 2015, Crustal-scale degassing due to magma system destabilization and magma-gas decoupling at Soufrière Hills Volcano, Montserrat: Geochemistry Geophysics Geosystems, v. 16, no. 9, p. 2797–2811, https://doi.org/10.1002/2015GC005791.

Chu, R., Helmberger, D.V., Sun, D., Jackson, J.M., and Zhu, L., 2010, Mushy magma beneath Yellowstone: Geophysical Research Letters, v. 37, L01306, https://doi.org/10.1029/2009GL041656.

Cinque, A., Rolandi, G., and Zamparelli, V., 1985, L'estensione dei depositi marini olocenici nei Campi Flegrei in relazione alla vulcano-tettonica: Bollettino della Società Geologica Italiana, v. 104, p. 327–348.

Clavero, J.E., Sparks, R.S.J., Pringle, M.S., Polanco, E., and Gardeweg, M.C., 2004, Evolution and volcanic hazards of Taapaca volcanic complex, central Andes of northern Chile: Journal of the Geological Society, v. 161, p. 603–618, https://doi.org/10.1144/0016-764902-065.

Cloos, M., 2001, Bubbling magma chambers, cupolas, and porphyry copper deposits: International Geology Review, v. 43, p. 285–311, https://doi.org/10.1080/00206810109465015.

Coira, B., Kay, S.M., and Viramonte, J., 1993, Upper Cenozoic magmatic evolution of the Argentine Puna—A model for changing subduction geometry: International Geology Review, v. 35, p. 677–720, https://doi.org/10.1080/00206819309465552.

Coleman, D.S., Gray, W., and Glazner, A.F., 2004, Rethinking the Emplacement and Evolution of Zoned Plutons: Geochronologic Evidence for Incremental Assembly of the Tuolumne Intrusive Suite: California Geology, v. 32, no. 5, p. 433–434, https://doi.org/10.1130/G20220.1.

Comeau, M.J., 2015, Electrical Resistivity Structure of the Altiplano-Puna Magma Body and Volcan Uturuncu from Magnetotelluric Data [Ph.D. thesis]: Edmonton, University of Alberta, 337 p.

Comeau, M.J., Unsworth, M.J., Ticona, F., and Sunagua, M., 2015, Magnetotelluric images of magma distribution beneath Volcán Uturuncu, Bolivia: Implications for magma dynamics: Geology, v. 43, no. 3, p. 243–246, https://doi.org/10.1130/G36258.1.

Comeau, M.J., Unsworth, M.J., and Cordell, D., 2016, New constraints on the magma distribution beneath Volcan Uturuncu, Bolivia from magnetotelluric data: Geosphere, v. 12, no. 5, p. 1391–1421, https://doi.org/10.1130/GES01277.1.

Delph, J.R., Ward, K.M., Zandt, G., Ducea, M.N., and Beck, S.L., 2017, Imaging a magma plumbing system from MASH zone to magma reservoir: Earth and Planetary Science Letters, v. 457, p. 313–324, https://doi.org/10.1016/j.epsl.2016.10.008.

del Potro, R., Diez, M., Blundy, J., Camacho, A.G., and Gottsmann, J., 2013, Diapiric ascent of silicic magma beneath the Bolivian Altiplano: Geophysical Research Letters, v. 40, p. 2044–2048, https://doi.org/10.1002/grl.50493.

de Silva, S.L., 1989, Altiplano-Puna volcanic complex of the Central Andes: Geology, v. 17, p. 1102–1106, https://doi.org/10.1130/0091-7613(1989)017<1102:APVCOT>2.3.CO;2.

de Silva, S.L., and Francis, P.W., 1991, Volcanoes of the Central Andes: Springer, New York, 216 p.

de Silva, S.L., and Gosnold, W.D., 2007, Episodic construction of batholiths: Insights from the spatiotemporal development of an ignimbrite flare-up: Journal of Volcanology and Geothermal Research, v. 167, no. 1, p. 320–335, https://doi.org/10.1016/j.jvolgeores.2007.07.015.

de Silva, S.L., and Gregg, P.M., 2014, Thermomechanical feedbacks in magmatic systems: Implications for growth, longevity, and evolution of large caldera-forming magma reservoirs and their supereruptions: Journal of Volcanology and Geothermal Research, v. 282, p. 77–91, https://doi.org/10.1016/j.jvolgeores.2014.06.001.

de Silva, S., Zandt, G., Trumbull, R., Viramonte, J.G., Salas, G., and Jiménez, N., 2006, Large ignimbrite eruptions and volcano-tectonic depressions in the Central Andes: A thermomechanical perspective, *in* Troise, C., De Natale, G., and Kilburn, C.R.J., eds., Mechanisms of Activity and Unrest at Large Calderas: Geological Society of London Special Publication 269, no. 1, p. 47–63, https://doi.org/10.1144/GSL.SP.2006.269.01.04.

de Silva, S.L., Mucek, A.E., Gregg, P.M., and Pratomo, I., 2015, Resurgent Toba—Field, chronologic, and model constraints on time scales and mechanisms of resurgence at large calderas: Frontiers in Earth Science, v. 3, p. 25, https://doi.org/10.3389/feart.2015.00025.

Devlin, S., Isacks, B.L., Pritchard, M.E., Barnhart, W.D., and Lohman, R.B., 2012, Depths and focal mechanisms of crustal earthquakes in the Central Andes determined from teleseismic waveform analysis and InSAR: Tectonics, v. 31, TC2002, https://doi.org/10.1029/2011TC002914.

Díaz, D., Heise, W., and Zamudio, F., 2015, Three-dimensional resistivity image of the magmatic system beneath Lastarria volcano and evidence for magmatic intrusion in the backarc (northern Chile): Geophysical Research Letters, v. 42, no. 13, p. 5212–5218, https://doi.org/10.1002/2015GL064426.

Dilles, J.H., and Wright, J.E., 1988, The chronology of early Mesozoic arc magmatism in the Yerington district of western Nevada and its regional implications: Geological Society of America Bulletin, v. 100, p. 644–652, https://doi.org/10.1130/0016-7606(1988)100<0644:TCOEMA>2.3.CO;2.

Driesner, T., and Heinrich, C.A., 2007, The system H_2O–NaCl. Part I: Correlation formulae for phase relations in temperature–pressure–composition space from 0 to 1000° C, 0 to 5000bar, and 0 to 1 X NaCl: Geochimica et Cosmochimica Acta, v. 71, no. 20, p. 4880–4901, https://doi.org/10.1016/j.gca.2006.01.033.

Druitt, T.H., Costa, F., Deloule, E., Dungan, M., and Scaillet, B., 2012, Decadal to monthly timescales of magma transfer and reservoir growth at a caldera volcano: Nature, v. 482, p. 77–80, https://doi.org/10.1038/nature10706.

Dvorkin, J.P., 2008, Yet another V_S equation: Geophysics, v. 73, p. E35–E39.

Einaudi, M.T., Hedenquist, J.W., and Inan, E.E., 2003, Sulfidation state of fluids in active and extinct hydrothermal systems: Transitions from porphyry to epithermal environments, *in* Simmons, S.F., and Graham, I., eds., Volcanic, Geothermal, and Ore-Forming Fluids: Rulers and Witnesses of Processes Within the Earth: Society of Economic Geologists and Geochemical Society Special Publication 10, p. 285–314.

Farrell, A., McNutt, S.R., and Thompson, G., 2017, Seismic attenuation, time delays and raypath bending of teleseisms beneath Cerro Uturuncu, Bolivia: Geosphere, v. 13, p. 699–722, https://doi.org/10.1130/GES01354.1.

Fialko, Y., and Pearse, J., 2012, Sombrero uplift above the Altiplano-Puna magma body: Evidence of a ballooning mid-crustal diapir: Science, v. 338, no. 6104, p. 250–252, https://doi.org/10.1126/science.1226358.

Fialko, Y., Simons, M., and Khazan, Y., 2001, Finite source modelling of magmatic unrest in Socorro, New Mexico, and Long Valley, California: Geophysical Journal International, v. 146, no. 1, p. 191–200, https://doi.org/10.1046/j.1365-246X.2001.00453.x.

Finnegan, N.J., and Pritchard, M.E., 2009, Magnitude and duration of surface uplift above the Socorro magma body: Geology, v. 37, no. 3, p. 231–234, https://doi.org/10.1130/G25132A.1.

Folkes, C.B., de Silva, S.L., Bindeman, I.N., and Cas, R.A., 2013, Tectonic and climate history influence the geochemistry of large-volume silicic magmas: New $\delta^{18}O$ data from the Central Andes with comparison to N America and Kamchatka: Journal of Volcanology and Geothermal Research, v. 262, p. 90–103, https://doi.org/10.1016/j.jvolgeores.2013.05.014.

Forsyth, D.W., 1993, Geophysical constraints on mantle flow and melt generation beneath mid-ocean ridges, *in* Morgan, J.P., Blackman, D.K., and Sinton, J.M., eds., American Geophysical Union Geophysical Monograph Series 71: Mantle Flow and Melt Generation at Mid-Ocean Ridges, p. 1–65.

Francis, P.W., O'Callaghan, L., Kretzschmar, G.A., Thorpe, R.S., Sparks, R.S.J., Page, R.N., de Barrio, R.E., Gillou, G., and Gonzalez, O.E., 1983, The Cerro Galán ignimbrite: Nature, v. 301, p. 51–53, https://doi.org/10.1038/301051a0.

Frank, M.R., Simon, A.C., Pettke, T., Candela, P.A., and Piccoli, P.M., 2011, Gold and copper partitioning in magmatic-hydrothermal systems at 800 °C and 100 MPa: Geochimica et Cosmochimica Acta, v. 75, p. 2470–2482, https://doi.org/10.1016/j.gca.2011.02.012.

Freymuth, H., Brandmeier, M., and Wörner, G., 2015, The origin and crust/mantle mass balance of Central Andean ignimbrite magmatism constrained by oxygen and strontium isotopes and erupted volumes: Contributions to Mineralogy and Petrology, v. 169, p. 1–24, https://doi.org/10.1007/s00410-015-1152-5.

Froger, J.-L., Rémy, D., Bonvalot, S., and Legrand, D., 2007, Two scales of inflation at Lastarria-Cordon del Azufre volcanic complex, Central Andes, revealed from ASAR-ENVISAT interferometric data: Earth and Planetary Science Letters, v. 255, p. 148–163, https://doi.org/10.1016/j.epsl.2006.12.012.

Fyfe, W.S., 1973, The granulite facies, partial melting and the Archaean crust: Philosophical Transactions of the Royal Society of London. Series A, Mathematical and Physical Sciences, v. 273, p. 457–461, https://doi.org/10.1098/rsta.1973.0011.

Gíslason, G., Eysteinsson, H., Björnsson, G., and Harðardóttir, V., 2015, Results of Surface Exploration in the Corbetti Geothermal Area, Ethiopia: Melbourne, Australia, Proceedings of the World Geothermal Congress, 10 p.

Glazner, A.F., Bartley, J.M., Coleman, D.S., Gray, W., and Taylor, R.Z., 2004, Are plutons assembled over millions of years by amalgamation from small magma chambers?: GSA Today, v. 14, p. 4–12, https://doi.org/10.1130/1052-5173(2004)014<0004:APAOMO>2.0.CO;2.

Gottsmann, J., Blundy, J., Henderson, S.T., Pritchard, M.E., and Sparks, R.S.J., 2017, Thermomechanical modeling of the Altiplano-Puna deformation anomaly: Multiparameter insights into magma mush reorganization: Geosphere, v. 13, p. 1042–1065, https://doi.org/10.1130/GES01420.1.

Gottsmann, J., del Potro, R., and Muller, C., 2018, 50 years of steady ground deformation in the Altiplano-Puna region of Southern Bolivia: Geosphere, v. 14, p. 65–73, https://doi.org/10.1130/GES01570.1.

Götze, H.-J., Lahmeyer, B., Schmidt, S., and Struck, S., 1994, The lithospheric structure of the Central Andes (20–26ES) as inferred from quantitative interpretation of regional gravity, *in* Reutter, K.-J., Scheuber, E., and Wigger, P.J., eds., Tectonics of the Southern Central Andes: Heidelberg, Springer, p. 7–21.

Grocke, S.B., de Silva, S.L., Iriarte, R., Lindsay, J.M., and Cottrell, E., 2017, Catastrophic caldera-forming (CCF) monotonous silicic magma reservoirs: Geochemical and petrological constraints on heterogeneity, magma dynamics, and eruption dynamics of the 3·49 Ma Tara Supereruption, Guacha II Caldera, SW Bolivia: Journal of Petrology, v. 58, no. 2, p. 227–260, https://doi.org/10.1093/petrology/egx012.

Grocke, S.B., de Silva, S.L., Wallace, P.J., Cottrell, E., and Schmitt, A.K., 2018, Catastrophic caldera-forming (CCF) monotonous silicic magma reservoirs: Constraints from volatiles in melt inclusions from the 3.49 Ma Tara Supereruption, Guacha II Caldera, SW Bolivia: Journal of Petrology, (in press) https://doi.org/10.1093/petrology/egy003.

Hacker, B.R., Ritzwoller, M.H., and Xie, J., 2014, Partially melted, mica-bearing crust in Central Tibet: Tectonics, v. 33, https://doi.org/10.1002/2014TC003545.

Hamilton, W., and Myers, W.B., 1967, The Nature of Batholiths: U.S. Geological Survey Professional Paper 554-C, p. C1–C30.

Hamling, I.J., Hreinsdóttir, S., Bannister, S., and Palmer, N., 2016, Off-axis magmatism along a subaerial back-arc rift: Observations from the Taupo Volcanic Zone, New Zealand: Science Advances, v. 2, no. 6, e1600288, https://doi.org/10.1126/sciadv.1600288.

Hammond, J.O.S., and Kendall, J.M., 2016, Constraints on melt distribution from seismology: A case study in Ethiopia, *in* Wright, T.J., Ayele, A., Ferguson, D.J., Kidane, T., and Vye-Brown, C., eds., Magmatic Rifting and Active Volcanism: Geological Society of London Special Publication 420, p. 127–147, https://doi.org/10.1144/SP420.14.

Hawkesworth, C.J., Hammill, M., Gledhill, A.R., van Calsteren, P., and Rogers, G., 1982, Isotope and trace element evidence for late-stage intra-crustal melting in the High Andes: Earth and Planetary Science Letters, v. 58, p. 240–254, https://doi.org/10.1016/0012-821X(82)90197-2.

Hedenquist, J.W., and Lowenstern, J.B., 1994, The role of magmas in the formation of hydrothermal ore deposits: Nature, v. 370, no. 6490, p. 519–527, https://doi.org/10.1038/370519a0.

Henderson, S.T., and Pritchard, M.E., 2013, Decadal volcanic deformation in the Central Andes Volcanic Zone revealed by InSAR time series: Geochemistry Geophysics Geosystems, v. 14, no. 5, p. 1358–1374, https://doi.org/10.1002/ggge.20074.

Henderson, S.T., and Pritchard, M.E., 2017, Time dependent deformation of Uturuncu Volcano, Bolivia constrained by GPS and InSAR measurements and implications for source models: Geosphere, v. 13, p. 1834–1854, https://doi.org/10.1130/GES01203.1.

Henderson, S.T., Delgado, F., Elliott, J., Pritchard, M.E., and Lundgren, P.R., 2017, Decelerating uplift at Lazufre volcanic center, Central Andes, from A.D. 2010 to 2016, and implications for geodetic models: Geosphere, v. 13, p. 1489–1505, https://doi.org/10.1130/GES01441.1.

Hickey, J., Gottsmann, J., and del Potro, R., 2013, The large-scale surface uplift in the Altiplano-Puna region of Bolivia: A parametric study of source characteristics and crustal rheology using finite element analysis: Geochemistry Geophysics Geosystems, v. 14, p. 540–555, https://doi.org/10.1002/ggge.20057.

Holtz, F., Sato, H., Lewis, J., Behrens, H., and Nakada, S., 2005, Experimental petrology of the 1991–1995 Unzen dacite, Japan. Part I: Phase relations, phase composition and pre-eruptive conditions: Journal of Petrology, v. 46, no. 2, p. 319–337, https://doi.org/10.1093/petrology/egh077.

Huang, H.H., Lin, F.C., Schmandt, B., Farrell, J., Smith, R.B., and Tsai, V.C., 2015, The Yellowstone magmatic system from the mantle plume to the upper crust: Science, v. 348, p. 773–776, https://doi.org/10.1126/science.aaa5648.

Hutchinson, L., 2015, Double-difference relocation of earthquakes at Uturuncu volcano, Bolivia, and Interior Alaska [M.S. thesis]: University of Alaska Fairbanks, 89 p.

Ingebritsen, S.E., Geiger, S., Hurwitz, S., and Driesner, T., 2010, Numerical simulation of magmatic hydrothermal systems: Reviews of Geophysics, v. 48, RG1002, 33 p.

Jackson, M. D., Cheadle, M. J. and Atherton, M. P., 2003, Quantitative modeling of granitic melt generation and segregation in the continental crust: Journal of Geophysical Research, v. 108, p. 2332–2353.

Jagoutz, O., and Behn, M.D., 2013, Foundering of lower island-arc crust as an explanation for the origin of the continental Moho: Nature, v. 504, no. 7478, p. 131–134, https://doi.org/10.1038/nature12758.

Jagoutz, O., and Schmidt, M.W., 2012, The formation and bulk composition of modern juvenile continental crust: The Kohistan arc: Chemical Geology, v. 298, p. 79–96, https://doi.org/10.1016/j.chemgeo.2011.10.022.

Jaxybulatov, K., Shapiro, N.M., Koulakov, I., Mordret, A., Landès, M., and Sens-Schönfelder, C., 2014, A large magmatic sill complex beneath the Toba caldera: Science, v. 346, p. 617–619, https://doi.org/10.1126/science.1258582.

Jay, J., Pritchard, M., West, M., Christensen, D., Haney, M., Minaya, E., Sunagua, M., McNutt, S., and Zabala, M., 2012, Shallow seismicity, triggered seismicity, and ambient noise tomography at the long-dormant Uturuncu Volcano, Bolivia: Bulletin of Volcanology, v. 74, p. 817–837, https://doi.org/10.1007/s00445-011-0568-7.

Jay, J., Costa, F., Pritchard, M., Lara, L., Singer, B., and Herrin, J., 2014, Locating magma reservoirs using InSAR and petrology before and during the 2011–2012 Cordón Caulle silicic eruption: Earth and Planetary Science Letters, v. 395, p. 254–266, https://doi.org/10.1016/j.epsl.2014.03.046.

Jay, J.A., Welch, M., Pritchard, M.E., Mares, P.J., Mnich, M.E., Melkonian, A.K., Aguilera, F., Naranjo, J.A., Sunagua, M., and Clavero, J., 2013, Volcanic hotspots of the central and southern Andes as seen from space by ASTER and MODVOLC between the years 2000 and 2010, *in* Pyle, D.M., Mather, T.A., and Biggs, J., eds., Remote Sensing of Volcanoes and Volcanic Processes: Integrating Observation and Modelling: Geological Society of London Special Publication 380, p. 161–185, https://doi.org/10.1144/SP380.1.

Jellinek, A.M., and DePaolo, D.J., 2003, A model for the origin of large silicic magma chambers: precursors of caldera-forming eruptions: Bulletin of Volcanology, v. 65, p. 363–381, https://doi.org/10.1007/s00445-003-0277-y.

Kaizuka, S., Newhall, C., Oyagi, N., and Yagi, H., 1989, Remarkable unrest at Iwo-jima caldera, Volcanic Islands, Japan: New Mexico Bureau of Mines and Mineral Resources Bulletin v. 13, 146 p.

Kay, S.M., and Coira, B.L., 2009, Shallowing and steepening subduction zones, continental lithospheric loss, magmatism, and crustal flow under the Central Andean Altiplano-Puna Plateau, *in* Kay, S.M., Ramos, V.A., and Dickinson, W.R., eds., Backbone of the Americas: Shallow Subduction, Plateau Uplift, and Ridge and Terrane Collision: Geological Society of America Memoir 204, p. 229–259., https://doi.org/10.1130/2009.1204(11).

Kennedy, B., Wilcock, J., and Stix, J., 2012, Caldera resurgence during magma replenishment and rejuvenation at Valles and Lake City calderas: Bulletin of Volcanology, v. 74, p.1833–1847, https://doi.org/10.1007/s00445-012-0641-x.

Kern, J.M., de Silva, S.L., Schmitt, A.K., Kaiser, J.F., Iriarte, A.R., and Economos, R., 2016, Geochronological imaging of an episodically constructed subvolcanic batholith: U-Pb in zircon chronochemistry of the Altiplano-Puna Volcanic Complex of the Central Andes: Geosphere, v. 12, p. 1054–1077, https://doi.org/10.1130/GES01258.1.

Kiser, E., Palomeras, I., Levander, A., Zelt, C., Harder, S., Schmandt, B., Hansen, S., Creager, K., and Ulberg, C., 2016, Magma reservoirs from the upper crust to the Moho inferred from high-resolution Vp and Vs models beneath Mount St. Helens, Washington State, USA: Geology, v. 44, p. 411–414, https://doi.org/10.1130/G37591.1.

Klemetti, E.W., and Grunder, A.L., 2008, Volcanic evolution of Volcán Aucanquilcha: A long-lived dacite volcano in the Central Andes of northern Chile: Bulletin of Volcanology, v. 70, p. 633–650, https://doi.org/10.1007/s00445-007-0158-x.

Kuang, X., and Jiao, J.J., 2014, An integrated permeability-depth model for Earth's crust: Geophysical Research Letters, v. 41, p. 7539–7545, https://doi.org/10.1002/2014GL061999.

Kukarina, E., West, M.E., Keyson, L.H., Koulakov, I., Tsibiov, L., and Smirnov, S., 2017, Focused magmatism beneath Uturuncu volcano: Insights from seismic tomography and deformation modeling: Geosphere, v. 13, p. 1855–1866, https://doi.org/10.1130/GES01403.1.

Lau, H.N., Tymofyeyeva, E., and Fialko, Y., 2017, Evidence of episodic crustal magmatic diapir and shallow volcanic activity at Uturuncu, Central Andes, from geodetic observations between 2014–2017: Fall meeting, American Geophysical Union, abstract V11C-0354.

Laumonier, M., Gaillard, F., and Sifre, D., 2015, The effect of pressure and water concentration on the electrical conductivity of dacitic melts: Implication for magnetotelluric imaging in subduction areas: Chemical Geology, v. 418, p. 66–76, https://doi.org/10.1016/j.chemgeo.2014.09.019.

Laumonier, M., Gaillard, F., Muir, D., Blundy, J., and Unsworth, M., 2017, Giant magmatic water reservoirs at mid-crustal depth inferred from electrical conductivity and the growth of the continental crust: Earth and Planetary Science Letters, v. 457, p. 173–180, https://doi.org/10.1016/j.epsl.2016.10.023.

Leidig, M., and Zandt, G., 2003, Modeling of highly anisotropic crust and application to the Altiplano-Puna volcanic complex of the Central Andes: Journal of Geophysical Research, v. 108, https://doi.org/10.1029/2001JB000649.

Lindsay, J.M., Schmitt, A.K., Trumbull, R.B., de Silva, S.L., Siebel, W., and Emmermann, R., 2001, Magmatic evolution of the La Pacana caldera system, Central Andes, Chile: Compositional variation of two cogenetic, large-volume felsic ignimbrites: Journal of Petrology, v. 42, no. 3, p. 459–486, https://doi.org/10.1093/petrology/42.3.459.

Lipman, P.W., 1984, The roots of ash-flow calderas in North America: windows into the tops of granitic batholiths: Journal of Geophysical Research, v. 89, p. 8801–8841, https://doi.org/10.1029/JB089iB10p08801.

Lipman, P.W., and Bachmann, O., 2015, Ignimbrites to batholiths: Integrating perspectives from geological, geophysical, and geochronological data: Geosphere, v. 11, no. 3, p. 705–743, https://doi.org/10.1130/GES01091.1.

Lopez, T., Aguilera, F., Tassi, F., Maarten de Moor, J., Bobrowski, N., Aiuppa, A., Tamburello, G., Rizzo, A., Liuzzo, M., Viveiros, F., Cardellini, C., Silva, C., Fisher, T., Jean-Baptiste, P., Kazahaya, R., Hidalgo, S., Lucic, G., Malowany, K., Bagnato, E., Bergsson, B., Reath, K., Liotta, M., and Chiodini, G., 2018, New constraints on the magmatic-hydrothermal system and volatile budget of Lastarria Volcano, Chile: Integrated results from the 2014 IAVCEI CCVG 12th Volcanic Gas Workshop: Geosphere, v. 14, https://doi.org/10.1130/GES01495.1.

Lucassen, F., Becchio, R., Harmon, R., Kasemann, S., Franz, G., Trumbull, R., Romer, R.L., and Dulski, P., 2001, Composition and density model of the continental crust in an active continental margin—The Central Andes between 21° and 27°S: Tectonophysics, v. 341, p. 195–223, https://doi.org/10.1016/S0040-1951(01)00188-3.

Lundstrom, C.C., and Glazner, A.F., 2016, Silicic Magmatism and the Volcanic-Plutonic Connection: Elements, v. 12, no. 2, p. 91–96, https://doi.org/10.2113/gselements.12.2.91.

Maher, S., 2017, Crustal anisotropy and state of stress at Uturuncu volcano, Bolivia, from shear-wave splitting measurements [M.S. thesis]: University of Bristol, 133 p.

McFarlin, H., Christensen, D.H., McNutt, S.R., Ward, K.M., Ryan, J., Zandt, G., and Thompson, G., 2018, Receiver function analysis of Uturuncu volcano, Bolivia and vicinity: Geosphere, v. 14, p. 50–64, https://doi.org.10.1130/GES01560.1.

McFarlin, H.L., Christensen, D.H., Thompson, G., McNutt, S.R., Ryan, J.C., Ward, K.M., Zandt, G., and West, M.E., 2014, Receiver function analyses of Uturuncu volcano, Bolivia and Lastarria/Cordón del Azufre volcanoes: American Geophysical Union, Fall meeting, abstract V31E-4792.

McKenzie, D., Jackson, J., and Priestley, K., 2005, Thermal structure of oceanic and continental lithosphere: Earth and Planetary Science Letters, v. 233, no. 3, p. 337–349, https://doi.org/10.1016/j.epsl.2005.02.005.

Michelfelder, G.S., 2015, The geochemical evolution of the Cerro Uturuncu magma chamber, sw Bolivia and its relation to the Andean Central Volcanic Zone [Ph.D. thesis]: Bozeman, Montana State University, 189 p., http://scholarworks.montana.edu/xmlui/handle/1/10142.

Michelfelder, G.S., Feeley, T.C., Wilder, A.D., and Klemetti, E.W., 2013, Modification of the continental crust by subduction zone magmatism and vice-versa: Across-strike geochemical variations of silicic lavas from individual eruptive centers in the Andean Central volcanic zone: Geosciences, v. 3, no. 4, p. 633–667, https://doi.org/10.3390/geosciences3040633.

Michelfelder, G.S., Feeley, T.C., and Wilder, A.D., 2014, The Volcanic Evolution of Cerro Uturuncu: A High-K, Composite Volcano in the Back-Arc of the Central Andes of SW Bolivia: International Journal of Geosciences, v. 5, no. 11, p. 1263, https://doi.org/10.4236/ijg.2014.511105.

Michelfelder, G.S., Wilder, A., Grunder, A., and Larson, P., 2016, Dedication: In memory of Todd Christian Feeley (1961–2015): Geosphere, https://doi.org/10.1130/GES01346.1.

Miller, C.F., Furbish, D.J., Walker, B.A., Claiborne, L.L., Koteas, G.C., Bleick, H.A., and Miller, J.S., 2011, Growth of plutons by incremental emplacement of sheets in crystal-rich host: evidence from Miocene intrusions of the Colorado River region, Nevada, USA: Tectonophysics, v. 500, no. 1, p. 65–77, https://doi.org/10.1016/j.tecto.2009.07.011.

Moorkamp, M., Heincke, B., Jegen, M., Roberts, A.W., and Hobbs, R.W., 2011, A framework for 3-D joint inversion of MT, gravity and seismic refraction data: Geophysical Journal International, v. 184, no. 1, p. 477–493, https://doi.org/10.1111/j.1365-246X.2010.04856.x.

Muir, D.D., 2013, Petrological and geochronological constraints on magma storage conditions beneath Uturuncu volcano, SW Bolivia [Ph.D. thesis]: University of Bristol, http://ethos.bl.uk/OrderDetails.do?uin=uk.bl.ethos.619259.

Muir, D.D., Blundy, J.D., Rust, A.C., and Hickey, J., 2014a, Experimental constraints on dacite pre-eruptive magma storage conditions beneath Uturuncu volcano: Journal of Petrology, v. 55, no. 4, p. 749–767, https://doi.org/10.1093/petrology/egu005.

Muir, D.D., Blundy, J.D., Hutchinson, M.C., and Rust, A.C., 2014b, Petrological imaging of an active pluton beneath Cerro Uturuncu, Bolivia: Contributions to Mineralogy and Petrology, v. 167, no. 3, article no. 980, p. 1–25, https://doi.org/10.1007/s00410-014-0980-z.

Muir, D.D., Barfod, D.N., and Blundy, J.D., 2015, The temporal record of magmatism at Cerro Uturuncu, Bolivian Altiplano, *in* Caricchi, L., and Blundy, J.D., eds., Chemical, Physical and Temporal Evolution of Magmatic Systems: Geological Society of London Special Publication 422, p. 57–83, https://doi.org/10.1144/SP422.1.

Mulcahy, P., Chen, C., Kay, S.M., Brown, L.D., Isacks, B.L., Sandvol, E., Heit, B., Yuan, X., and Coira, B.L., 2014, Central Andean mantle and crustal seismicity beneath the Southern Puna plateau and the northern margin of the Chilean-Pampean flat slab: Tectonics, v. 33, https://doi.org/10.1002/2013TC003393.

Müntener, O., and Ulmer, P., 2006, Experimentally derived high-pressure cumulates from hydrous arc magmas and consequences for the seismic velocity structure of lower arc crust: Geophysical Research Letters, v. 33, L21308, https://doi.org/10.1029/2006GL027629.

Nandedkar, R.H., Ulmer, P., and Müntener, O., 2014, Fractional crystallization of primitive, hydrous arc magmas: an experimental study at 0.7 GPa: Contributions to Mineralogy and Petrology, v. 167, no. 6, article no. 1015, p. 1–27, https://doi.org/10.1007/s00410-014-1015-5.

Naranjo, J.A., 1985, Sulphur flows at Lastarria volcano in the North Chilean Andes: Nature, v. 313, p. 778–780, https://doi.org/10.1038/313778a0.

Naranjo, J.A., 1988, Coladas de azufre de los volcanes Lastarria y Bayo en el norte de Chile: reología, génesis e importancia en geología planetaria: Revista Geológica de Chile, v. 15, no. 1, p. 3–12.

Naranjo, J.A., 2010, Geología del Complejo Volcánico Lastarria, Región de Antofagasta. Servicio Nacional de Geología y Minería, Carta Geológica de Chile, Serie Geología Básica, No. 123, 1:25,000 scale, 1 sheet, 33 p. text.

Naranjo, J.A., and Cornejo, P., 1992, Hoja Salar de la Isla. Servicio Nacional de Geología y Minería, Carta Geológica de Chile, No. 72, 1:250.000 scale, 1 sheet.

Naranjo, J.A., Villa, V., and Venegas, C., 2013, Geología de las áreas Salar de Pajonales y Cerro Moño, regiones de Antofagasta y Atacama. Servicio Nacional de Geología y Minería, Carta Geológica de Chile, Serie Geología Básica, nos. 153 and 154, scale 1:100.000, 1 sheet, 72 p. text.

Naranjo, J.A., Villa, V., Ramírez, C., and Pérez de Arce, C., 2018a, Volcanism and tectonics in the southern Central Andes: Tempo, styles and relationships: Geosphere, v. 14, https://doi.org/10.1130/GES01350.1.

Naranjo, J.A., Hevia, F., Villa, V., and Ramírez, C., 2018b, Miocene to recent geological evolution of the Lazufre segment in the Andean volcanic arc: Geosphere, v. 14, https://doi.org/10.1130/GES01352.1.

Nikkhoo, M., Walter, T.R., Lundgren, P., Spica, Z., and Legrand, D., 2016, Stress interaction at the Lazufre volcanic region, as constrained by InSAR, seismic tomography and boundary element modelling: European Geosciences Union General Assembly Conference, v. 18, p. 16,121.

Ort, M., Coira, B., and Mazzoni, M., 1996, Generation of a crust-mantle magma mixture: Magma sources and contamination at Cerro Panizos, Central Andes: Contributions to Mineralogy and Petrology, v. 123, p. 308–322, https://doi.org/10.1007/s004100050158.

Parker, A.L., Biggs, J., and Lu, Z., 2014, Investigating long-term subsidence at Medicine Lake Volcano, CA, using multitemporal InSAR: Geophysical Journal International, v. 199, p. 844–859, https://doi.org/10.1093/gji/ggu304.

Paterson, S.R., Okaya, D., Memeti, V., Economos, R., and Miller, R.B., 2011, Magma addition and flux calculations of incrementally constructed magma chambers in continental margin arcs: Combined field, geochronologic, and thermal modeling studies: Geosphere, v. 7, p. 1439–1468, https://doi.org/10.1130/GES00696.1.

Paulatto, M., Annen, C., Henstock, T.J., Kiddle, E., Minshull, T.A., Sparks, R.S.J., and Voight, B., 2012, Magma chamber properties from integrated seismic tomography and thermal modeling at Montserrat: Geochemistry Geophysics Geosystems, v. 13, Q01014, https://doi.org/10.1029/2011GC003892.

Pearse, J., and Fialko, Y., 2010, Mechanics of active magmatic intraplating in the Rio Grande Rift near Socorro, New Mexico: Journal of Geophysical Research. Solid Earth, v. 115, B07413, https://doi.org10.1029/2009JB006592.

Pearse, J., and Lundgren, P., 2013, Source model of deformation at Lazufre volcanic center, central Andes, constrained by InSAR time series: Geophysical Research Letters, v. 40, p. 1059–1064, https://doi.org/10.1002/grl.50276.

Perkins, J.P., Finnegan, N.J., Henderson, S.T., and Rittenour, T.M., 2016a, Topographic constraints on magma accumulation below the actively uplifting Uturuncu and Lazufre volcanic centers in the Central Andes: Geosphere, v. 12, p. 1078–1096, https://doi.org/10.1130/GES01278.1.

Perkins, J.P., Ward, K.M., de Silva, S.L., Zandt, G., Beck, S.L., and Finnegan, N.J., 2016b, Surface uplift in the Central Andes driven by growth of the Altiplano Puna Magma Body: Nature Communications, v. 7, article no. 13185, p. 1–10, https://doi.org/10.1038/ncomms13185.

Pierce, K.L., Cannon, K.P., Meyer, G.A., and Trebesch, M.J., 2002, Post-glacial inflation-deflation cycles, tilting, and faulting in the Yellowstone caldera based on Yellowstone Lake shorelines: U.S. Geological Survey Open-File Report 2002-142, 30 p.

Pommier, A., and Garnero, E.J., 2014, Petrology-based modeling of mantle melt electrical conductivity and joint interpretation of electromagnetic and seismic results: Journal of Geophysical Research. Solid Earth, v. 119, p. 4001–4016, https://doi.org/10.1002/2013JB010449.

Pommier, A., Leinenweber, K., Kohlstedt, D.L., Qi, C., Garnero, E.J., Mackwell, S.J., and Tyburczy, J.A., 2015, Experimental constraints on the electrical anisotropy of the lithosphere-asthenosphere system: Nature, v. 522, no. 7555, p. 202, https://doi.org/10.1038/nature14502.

Prezzi, C.B., Götze, H.J., and Schmidt, S., 2009, 3D density model of the Central Andes: Physics of the Earth and Planetary Interiors, v. 177, p. 217–234, https://doi.org/10.1016/j.pepi.2009.09.004.

Priestley, K., and McKenzie, D., 2013, The relationship between shear wave velocity, temperature, attenuation and viscosity in the shallow part of the mantle: Earth and Planetary Science Letters, v. 381, p. 78–91, https://doi.org/10.1016/j.epsl.2013.08.022.

Pritchard, M.E., and Gregg, P.M., 2016, Geophysical Evidence for Silicic Crustal Melt in the Continents: Where, What Kind, and How Much?: Elements, v. 12, no. 2, p. 121–127, https://doi.org/10.2113/gselements.12.2.121.

Pritchard, M.E., and Simons, M., 2002, A satellite geodetic survey of large-scale deformation of volcanic centres in the Central Andes: Nature, v. 418, no. 6894, p. 167–171, https://doi.org/10.1038/nature00872.

Pritchard, M.E., and Simons, M., 2004, An InSAR-based survey of volcanic deformation in the Central Andes: Geochemistry Geophysics Geosystems, v. 5, Q02002, https://doi.org/10.1029/2003GC000610.

Pritchard, M.E., Rubin, A.M., and Wolfe, C.J., 2007, Do flexural stresses explain the mantle fault zone beneath Kilauea, Hawaii?: Geophysical Journal International, v. 168, p. 419–430, https://doi.org/10.1111/j.1365-246X.2006.03169.x.

Pritchard, M.E., Henderson, S.T., Jay, J.A., Soler, V., Krzesni, D.A., Button, N.E., Welch, M.D., Semple, A.G., Glass, B., Sunagua, M., and Minaya, E., 2014a, Reconnaissance earthquake studies at nine volcanic areas of the Central Andes with coincident satellite thermal and InSAR observations: Journal of Volcanology and Geothermal Research, v. 280, p. 90–103, https://doi.org/10.1016/j.jvolgeores.2014.05.004.

Pritchard, M.E., Furtney, M., and Cooper, J., 2014b, Is a Zombie Volcano a Thing?: American Geophysical Union, Volcanology, Geochemistry, and Petrology Education and Outreach Spotlight, http://vgp.agu.org/vgp-spotlight-is-a-zombie-volcano-a-thing.

Remy, D., Froger, J.L., Perfettini, H., Bonvalot, S., Gabalda, G., Albino, F., Cayol, V., Legrand, D., and De Saint Blanquat, M., 2014, Persistent uplift of the Lazufre volcanic complex (Central Andes): New insights from PCAIM inversion of InSAR time series and GPS data: Geochemistry Geophysics Geosystems, v. 15, no. 9, p. 3591–3611, https://doi.org/10.1002/2014GC005370.

Richards, J.P., and Villeneuve, M., 2002, Characteristics of late Cenozoic volcanism along the Archibarca lineament from Cerro Llullaillaco to Corrida de Cori, northwest Argentina: Journal of Volcanology and Geothermal Research, v. 116, p. 161–200, https://doi.org/10.1016/S0377-0273(01)00329-8.

Roman, A.M., and Jaupart, C., 2016, Fate of mafic and ultramafic intrusions in the continental crust: Earth and Planetary Science Letters, v. 453, p. 131–140, https://doi.org/10.1016/j.epsl.2016.07.048.

Ruch, J., and Walter, T.R., 2010, Relationship between the InSAR-measured uplift, the structural framework, and the present-day stress field at Lazufre volcanic area, Central Andes: Tectonophysics, v. 492, p. 133–140, https://doi.org/10.1016/j.tecto.2010.06.003.

Ruch, J., Anderssohn, J., Walter, T.R., and Motagh, M., 2008, Caldera-scale inflation of the Lazufre volcanic area, South America: Evidence from InSAR: Journal of Volcanology and Geothermal Research, v. 174, p. 337–344, https://doi.org/10.1016/j.jvolgeores.2008.03.009.

Ruch, J., Manconi, A., Zeni, G., Solaro, G., Pepe, A., Shirzaei, M., Walter, T.R., and Lanari, R., 2009, Stress transfer in the Lazufre volcanic area, central Andes: Geophysical Research Letters, v. 36, L22303, https://doi.org/10.1029/2009GL041276.

Saibi, H., Aboud, E., and Gottsmann, J., 2015, Curie point depth from spectral analysis of aeromagnetic data for geothermal reconnaissance in Afghanistan: Journal of African Earth Sciences, v. 111, p. 92–99, https://doi.org/10.1016/j.jafrearsci.2015.07.019.

Schilling, F.R., Trumbull, R.B., Brasse, H., Haberland, C., Asch, G., Bruhn, D., Mai, K., Haak, V., Giese, P., Muñoz, M., and Ramelow, J., 2006, Partial melting in the Central Andean crust: A review of geophysical, petrophysical, and petrologic evidence, *in* Oncken, O., Chong, G., Franz, G., Giese, P., Götze, H.-J., Ramos, V.A., Strecker, M.R., and Wigger, P., eds., The Andes: Active Subduction Orogeny: Berlin, Heidelberg, Springer, p. 459–474, https://doi.org/10.1007/978-3-540-48684-8_22.

Schmitt, A.K., de Silva, S.L., Trumbull, R., and Emmermann, R., 2001, Magma evolution in the Purico ignimbrite complex, northern Chile: Evidence for zoning of a dacitic magma by injection of rhyolitic melts following mafic recharge: Contributions to Mineralogy and Petrology, v. 140, p. 680–700, https://doi.org/10.1007/s004100000214.

Schmitt, A.K., Lindsay, J.M., de Silva, S.L., and Trumbull, R.B., 2003, U–Pb Zircon Chronostratigraphy of Early-Pliocene ignimbrites from La Pacana, north Chile: Implications for the formation of stratified magma chambers: Journal of Volcanology and Geothermal Research, v. 120, p. 43–53, https://doi.org/10.1016/S0377-0273(02)00359-1.

Schmitz, M., Heinsohn, W.D., and Schilling, F.R., 1997, Seismic, gravity and petrological evidence for partial melt beneath the thickened central Andean crust (21–23 S): Tectonophysics, v. 270, p. 313–326.

Shen, W., Alvizuri, C., Lin, F.-C., and Tape, C., 2017, A one-dimensional seismic model for Uturuncu volcano, Bolivia, and its impact on full moment tensor inversions: Geosphere, v. 13, p. 1–10, https://doi.org/10.1130/GES01353.1.

Sillitoe, R.H., 2010, Porphyry copper systems: Economic Geology and the Bulletin of the Society of Economic Geologists, v. 105, p. 3–41, https://doi.org/10.2113/gsecongeo.105.1.3.

Simon, A.C., Pettke, T., Candela, P.A., Piccolli, P.M., and Heinrich, C.A., 2006, Copper partitioning in a melt-vapor-brine-magnetite-pyrrhotite assemblage: Geochimica et Cosmochimica Acta, v. 70, no. 22, p. 5583–5600, https://doi.org/10.1016/j.gca.2006.08.045.

Sims, N.E., Christensen, D.H., and Moore-Driskell, M.M., 2015, Shear wave splitting observations beneath Uturuncu volcano, Bolivia: American Geophysical Union, Fall Meeting, abstract DI21A-2588.

Singer, B.S., Tikoff, B., Le Mével, H., Anderson, N.L., Cordova, L., and Licciardi, J.M., 2015, Linking modern, rapid, surface uplift at the Laguna del Maule volcanic field, Chilean Andes, to rhyolitic magma-driven uplift spanning the Holocene: American Geophysical Union, Fall Meeting, v. G31, p. C-04.

Smith, R.B., Jordan, M., Steinberger, B., Puskas, C.M., Farrell, J., Waite, G.P., Husen, S., Chang, W.L., and O'Connell, R., 2009, Geodynamics of the Yellowstone hotspot and mantle plume: Seismic and GPS imaging, kinematics, and mantle flow: Journal of Volcanology and Geothermal Research, v. 188, p. 26–56, https://doi.org/10.1016/j.jvolgeores.2009.08.020.

Solano, J., Jackson, M.D., Sparks, R.S.J., and Blundy, J.D., 2014, Evolution of major and trace element composition during melt migration through crystalline mush: Implications for chemical differentiation in the crust: American Journal of Science, v. 314, p. 895–939, https://doi.org/10.2475/05.2014.01.

Solano, J.M.S., Jackson, M.D., Sparks, R.S.J., Blundy, J.D., and Annen, C., 2012, Segregation in deep crustal hot zones: A mechanism for chemical differentiation, crustal assimilation and the formation of evolved magmas: Journal of Petrology, v. 53, p. 1999–2026, https://doi.org/10.1093/petrology/egs041.

Sparks, R.S.J., and Cashman, K.V., 2017, Dynamic magma systems: Implications for forecasting volcanic activity: Elements, v. 13, no. 1, p. 35–40, https://doi.org/10.2113/gselements.13.1.35.

Sparks, R.S.J., Folkes, C.B., Humphreys, M.C.S., Barfod, D.N., Clavero, J., Sunagua, M.C., McNutt, S.R., and Pritchard, M.E., 2008, Uturuncu volcano, Bolivia: Volcanic unrest due to mid-crustal magma intrusion: American Journal of Science, v. 308, p. 727–769, https://doi.org/10.2475/06.2008.01.

Spica, Z., Legrand, D., Mendoza, A., Dahn, T., Walter, T.R., Heimann, S., Froger, J.-L., and Rémy, D., 2012, Analysis of surface waves extracted from seismic noise for the Lastarria volcanic zone, Chile: Colima, México, Cities on Volcanoes 7: International Association of Volcanology and Chemistry of the Earth's Interior, abstract 4C1.4-17.

Spica, Z., Legrand, D., Iglesias, A., Walter, T.R., Heimann, S., Dahm, T., Froger, J.-L., Rémy, D., Bonvalot, S., West, M., and Pardo, M., 2015, Hydrothermal and magmatic reservoirs at Lazufre volcanic area, revealed by a high-resolution seismic noise tomography: Earth and Planetary Science Letters, v. 421, p. 27–38, https://doi.org/10.1016/j.epsl.2015.03.042.

Spica, Z., Perton, M., and Legrand, D., 2017, Anatomy of the Colima magmatic system, Mexico: Earth and Planetary Science Letters, v. 459, p. 1–13, https://doi.org/10.1016/j.epsl.2016.11.010.

Stechern, A., Just, T., Holtz, F., Blume-Oeste, M., and Namur, O., 2017, Decoding magma plumbing and geochemical evolution beneath the Lastarria volcanic complex (Northern Chile)—Evidence for multiple magma storage regions: Journal of Volcanology and Geothermal Research, v. 338, p. 25–45, https://doi.org/10.1016/j.jvolgeores.2017.03.018.

Sunagua, M., 2004, Amenaza volcánica en la region del volcán Uturuncu–Provincia Sud Lípez del Departamento de Potosí [Tesis de Grado]: Potosí, Bolivia, Universidad Autónoma Tomás Frías.

Tamburello, G., Hansteen, T.H., Bredemeyer, S., Aiuppa, A., and Tassi, F., 2014, Gas emissions from five volcanoes in northern Chile and implications for the volatiles budget of the Central Volcanic Zone: Geophysical Research Letters, v. 41, p. 4961–4969, https://doi.org/10.1002/2014GL060653.

Tattitch, B., and Blundy, J., 2017, Partitioning of Cu and Mo between felsic melts and saline magmatic fluids: Influence of salinity, fO_2 and fS_2: Transactions of the Institution of Mining and Metallurgy Section B. Applied Earth Science, v. 126, p. 99.

Tattitch, B.C., Candela, P.A., Piccoli, P.M., and Bodnar, R.J., 2015, Copper partitioning between felsic melt and H_2O-CO_2 bearing saline fluids: Geochimica et Cosmochimica Acta, v. 148, p. 81–99, https://doi.org/10.1016/j.gca.2014.08.025.

Tierney, C.R., Schmitt, A.K., Lovera, O.M., and de Silva, S.L., 2016, Voluminous plutonism during volcanic quiescence revealed by thermochemical modeling of zircon: Geology, v. 44, p. 683–686, https://doi.org/10.1130/G37968.1.

Unsworth, M., and Rondenay, S., 2013, Mapping the distribution of fluids in the crust and lithospheric mantle utilizing geophysical methods, *in* Harlov, D., and Austrheim, H., eds., Metasomatism and the Chemical Transformation of Rock: Berlin, Heidelberg, Springer, p. 535–598, https://doi.org/10.1007/978-3-642-28394-9_13.

Ussher, G., Harvey, C., Johnstone, R., and Anderson, E., 2000, Understanding the resistivities observed in geothermal systems: Proceedings World Geothermal Congress, Kyushu–Tohoku, Japan, p. 1915–1920.

Vaughan, R.G., Keszthelyi, L.P., Lowenstern, J.B., Jaworowski, C., and Heasler, H., 2012, Use of ASTER and MODIS thermal infrared data to quantify heat flow and hydrothermal change at Yellowstone National Park: Journal of Volcanology and Geothermal Research, v. 233, p. 72–89, https://doi.org/10.1016/j.jvolgeores.2012.04.022.

Walter, T.R., and Motagh, M., 2014, Deflation and inflation of a large magma body beneath Uturuncu volcano, Bolivia?: Insights from InSAR data, surface lineaments and stress modelling: Geophysical Journal International, v. 198, p. 462–473, https://doi.org/10.1093/gji/ggu080.

Ward, K.M., Porter, R.C., Zandt, G., Beck, S.L., Wagner, L.S., Minaya, E., and Tavera, H., 2013, Ambient noise tomography across the Central Andes: Geophysical Journal International, v. 194, p. 1559–1573, https://doi.org/10.1093/gji/ggt166.

Ward, K.M., Porter, R.C., Zandt, G., Beck, S.L., Wagner, L.S., Minaya, E., and Tavera, H., 2014a, Erratum: ambient noise tomography across the Central Andes: Geophysical Journal International, v. 196, p. 1264–1265, https://doi.org/10.1093/gji/ggt429.

Ward, K.M., Zandt, G., Beck, S.L., Christensen, D.H., and McFarlin, H., 2014b, Seismic imaging of the magmatic underpinnings beneath the Altiplano-Puna volcanic complex from the joint inversion of surface wave dispersion and receiver functions: Earth and Planetary Science Letters, v. 404, p. 43–53, https://doi.org/10.1016/j.epsl.2014.07.022.

Ward, K.M., Delph, J.R., Zandt, G., Beck, S.L., and Ducea, M.N., 2017, Magmatic evolution of a Cordilleran flare-up and its role in the creation of silicic crust: Scientific Reports, v. 7, no. 9047, p. 1–8, https://doi.org/10.1038/s41598-017-09015-5.

Weis, P., 2015, The dynamic interplay between saline fluid flow and rock permeability in magmatic-hydrothermal systems: Geofluids, v. 15, p. 350–371, https://doi.org/10.1111/gfl.12100.

Wicks, C.W., Thatcher, W., Dzurisin, D., and Svarc, J., 2006, Uplift, thermal unrest and magma intrusion at Yellowstone caldera: Nature, v. 440, no. 7080, p. 72–75, https://doi.org/10.1038/nature04507.

Wilder, A.D., 2015, Petrology and geochemistry of the Lazufre volcanic complex: evidence for diverse petrogenetic processes and sources in the Andean Central Volcanic Zone [M.S. thesis]: Bozeman, Montana State University, 134 p., http://scholarworks.montana.edu/xmlui/handle/1/10164.

Yuan, X., Sobolev, S.V., Kind, R., Oncken, O., Bock, G., Asch, G., Schurr, B., Graeber, F., Rudloff, A., Hanka, W., and Wylegalla, K., 2000, Subduction and collision processes in the Central Andes constrained by converted seismic phases: Nature, v. 408, no. 6815, p. 958–961, https://doi.org/10.1038/35050073.

Zajacz, Z., Seo, J.H., Candela, P.A., Piccoli, P.M., and Tossell, J.A., 2011, The solubility of copper in high-temperature magmatic vapors: A quest for the significance of various chloride and sulfide complexes: Geochimica et Cosmochimica Acta, v. 75, p. 2811–2827, https://doi.org/10.1016/j.gca.2011.02.029.

Zandt, G., Leidig, M., Chmielowski, J., and Baumont, D., 2003, Seismic detection and character-ization of the Altiplano-Puna magma body, Central Andes: Pure and Applied Geophysics, v. 160, p. 789–807, https://doi.org/10.1007/PL00012557.

Zimmer, M., Walter, T.R., Kujawa, C., Gaete, A., and Franco-Marin, L., 2017, Thermal and gas dynamic investigations at Lastarria volcano, Northern Chile. The influence of precipitation and atmospheric pressure on the fumarole temperature and the gas velocity: Journal of Volcanology and Geothermal Research, v. 346, p. 134–140, https://doi.org/10.1016/j.jvolgeores.2017.03.013.